



HAL
open science

Natural antisense transcription of presenilin in sea urchin reveals a possible role for natural antisense transcription in the general control of gene expression during development

Odile Bronchain, Bertrand Ducos, Harald Putzer, Marine Delagrangé, Soumaya Laalami, Laetitia Philippe-Caraty, Krystel Saroul, Brigitte Ciapa

► To cite this version:

Odile Bronchain, Bertrand Ducos, Harald Putzer, Marine Delagrangé, Soumaya Laalami, et al.. Natural antisense transcription of presenilin in sea urchin reveals a possible role for natural antisense transcription in the general control of gene expression during development. *Journal of Cell Science*, 2023, 136 (14), pp.jcs26128. 10.1242/jcs.261284 . hal-04235467

HAL Id: hal-04235467

<https://cnrs.hal.science/hal-04235467v1>

Submitted on 10 Oct 2023

HAL is a multi-disciplinary open access archive for the deposit and dissemination of scientific research documents, whether they are published or not. The documents may come from teaching and research institutions in France or abroad, or from public or private research centers.

L'archive ouverte pluridisciplinaire **HAL**, est destinée au dépôt et à la diffusion de documents scientifiques de niveau recherche, publiés ou non, émanant des établissements d'enseignement et de recherche français ou étrangers, des laboratoires publics ou privés.



Distributed under a Creative Commons Attribution 4.0 International License

RESEARCH ARTICLE

Natural antisense transcription of presenilin in sea urchin reveals a possible role for natural antisense transcription in the general control of gene expression during development

Odile Bronchain¹, Bertrand Ducos², Harald Putzer³, Marine Delagrance², Soumaya Laalami³, Laetitia Philippe-Caraty⁴, Krystal Saroul⁵ and Brigitte Ciapa^{1,*}

ABSTRACT

One presenilin gene (*PSEN*) is expressed in the sea urchin embryo, in the vegetal pole of the gastrula and then mainly in cilia cells located around the digestive system of the pluteus, as we recently have reported. *PSEN* expression must be accurately regulated for correct execution of these two steps of development. While investigating *PSEN* expression changes in embryos after expansion of endoderm with LiCl or of ectoderm with Zn²⁺ by whole-mount *in situ* hybridization (WISH) and quantitative PCR (qPCR), we detected natural antisense transcription of *PSEN*. We then found that *Endo16* and *Wnt5*, markers of endo-mesoderm, and of *Hnf6* and *Gsc*, markers of ectoderm, are also sense and antisense transcribed. We discuss that general gene expression could depend on both sense and antisense transcription. This mechanism, together with the *PSEN* gene, should be included in gene regulatory networks (GRNs) that theorize diverse processes in this species. We suggest that it would also be relevant to investigate natural antisense transcription of *PSEN* in the field of Alzheimer's disease (AD) where the role of human *PSEN1* and *PSEN2* is well known.

KEY WORDS: Presenilin, PSEN, Natural antisense transcription, Sea urchin, Development, Endo16, Wnt5, Hnf6, Goosecoid, Gsc, Alzheimer's disease, LiCl, Zn²⁺

INTRODUCTION


A precise control of gene expression is required for the formation of tissues and organs in the right place and at the right time in order to result in the correct development of any multicellular organism. The sea urchin has been, for tens of years, a remarkable model to study gene regulatory mechanisms that underlie early embryogenesis. Several gene regulatory networks (GRNs) have been constructed and are used to theorize diverse developmental processes in this species, such as cell type differentiation, cell migration, morphogenesis, etc.

(Cary et al., 2020; Erkenbrack et al., 2018; Peter and Davidson, 2017). GRNs have also been designed in various other biological models including animals, such as *Xenopus*, in plants, and in cancer cells etc. GRNs are conventionally represented as printed circuit diagrams where networks of regulatory genes encoding transcription factors and signaling molecules interact with each other through switches, feedforward and feedback loops and they affect other genes expressed downstream of these regulators (McDonald and Reed, 2022). Among the most-detailed GRNs in the sea urchin are, for example, those deciphering the endomesoderm development (Sethi et al., 2009) and the onset of gastrulation (Ettensohn, 2020). These circuit diagrams, where positive and negative feedbacks have been hypothesized by statistical calculations, have become more and more sophisticated with time, with them being modeled by Boolean analysis and bound to cell and tissue movements (Istrail and Peter, 2019). Very recently, developmental GRNs established in *Strongylocentrotus purpuratus* have been compared to single-cell RNA-seq datasets that were obtained at different times of *Lytechinus variegatus* development and linked to computational methods to trace lineage diversifications (Wang et al., 2019). This study has enabled the highlighting of some of the limits in the interpretation of GRNs. For example, only transcription factors that are known at a defined time are considered in those GRN pathways, specification within some cell lineages does not necessarily occur synchronously in a define tissue, and expression of genes that are expressed either ubiquitously or in different lineages seems to be elusive. Finally, and as we discuss below, some crucial regulation processes that function from the start of transcription to post-transcriptional control mechanisms, in order make sure that the protein corresponding to a specific gene is produced, have not been taken into account. Therefore, although these complicated diagrams give a great image of the complexity of the embryonic development, they might well only represent the visible tip of a gigantic iceberg.

In the studies that have led to the building of GRNs, the expression of genes is most often measured by whole-mount *in situ* hybridization (WISH) (Erkenbrack et al., 2018, 2019), microarray technology and quantitative (q)PCR. Firstly, the results that are given in GRNs by these methods are the expression of sense transcripts that might not necessarily be full length. Although well known to be crucial during cell differentiation and development in various biological models, post-transcriptional steps such as alternative splicing, mRNA trafficking and localization or mRNA stability and decay have not been taken into account in GRNs (Corbett, 2018; Halbeisen et al., 2008). Secondly, it has been known for decades that the level of a given mRNA does not necessarily match that of its corresponding protein and thus cannot explain genotype–phenotype relationships, which has now been confirmed by systematic studies quantifying transcripts and proteins at the genomic scale. Several processes

¹Paris-Saclay Institute of Neuroscience, CNRS, UMR CNRS 9197, Université Paris-Saclay, 75005 Paris, France. ²High Throughput qPCR Core Facility of the ENS, Université PSL, IBENS, Laboratoire de Physique de l'Ecole normale supérieure, ENS, Université PSL, CNRS, Sorbonne Université, Université de Paris, 75005 Paris, France. ³CNRS, Université Paris Cité, Expression Génétique Microbienne, IBPC, 75005 Paris, France. ⁴Institute for Integrative Biology of the Cell (I2BC), CEA, CNRS, Univ. Paris-Sud, Université Paris-Saclay, 91190 Gif-sur-Yvette, France. ⁵Institut CURIE, Université Paris-Saclay, INSERM U932, Immunité et Cancer, 91400 Orsay, France.

*Author for correspondence (brigitte.ciapa@universite-paris-saclay.fr)

 B.D., 0000-0002-5322-1339; H.P., 0000-0002-3354-4616; B.C., 0000-0002-3794-6209

Handling Editor: David Glover
Received 26 April 2023; Accepted 7 June 2023

beyond transcription, involved in the modulation of translation rates or of protein half-life, in protein synthesis delay or in protein transport and location, lead to precise levels of functional proteins (Liu et al., 2016). Thirdly, RNA transcripts that are translated into proteins represent only a very small percentage of the genome (2–3% in humans, ~20% in *Drosophila*), whereas the percentage of non-coding RNAs (ncRNAs) is huge, representing ~70% of the human genome. Some of these ncRNAs have indeed been known for a long time, given that they are constitutively expressed and essential for protein translation. They comprise the small nuclear RNAs (snRNAs), which are mainly involved in splicing events, the transfer RNAs (tRNAs), which decode the mRNA sequence into peptide or protein, and the ribosomal RNAs (rRNAs), thought to represent the most abundant RNA molecules in the cell (Fu, 2014). But over the past 30 years the large family of natural antisense transcripts (NATs) (Krappinger et al., 2021; Zhao et al., 2020) has also emerged. These transcripts are generated from the strand opposite to that of the sense transcript of both protein-coding and nonprotein-coding genes and have been classified either as short ncRNAs (<200 nucleotides in length) or as long ncRNAs (lncRNAs, >200 nucleotides in length). The short ncRNAs include the piwi-associated RNAs, the endogenous short-interfering RNAs (siRNAs) and the microRNAs (miRNAs), which are all already accepted as fundamental players in gene regulation. As for lncRNAs, their number is constantly growing (several thousand have been identified so far in humans). It is known that they can not only form from antisense transcription but also from sense transcription, and they are being recognized as more and more essential for many biological processes, including, cell signal transduction, immune response, cell proliferation and differentiation. Their abnormal expression is therefore now linked to a variety of diseases including cancers or neurodegenerative diseases (Yao et al., 2019). lncRNAs are now often classified according to their position in the genome relative to the target protein-coding gene. They can be partially or completely complementary to a given mRNA on the opposite strand, produced from the enhancer region or a promoter of a protein-coding gene, or formed from the introns of genes or large intergenic regions. They are given increasingly important roles, for example, in epigenetic regulation and sequestration of miRNAs, in splicing processes, during transcription and in protein translation, which they can either activate or inhibit (Statello et al., 2021).

In conclusion, all these control mechanisms might well cause modifications in gene expression displayed in GRNs and represent the ‘submerged’ part of the gigantic iceberg referred to above.

We became interested in all of these questions after our last published study concerning the expression of presenilin (*PSEN*) in the sea urchin embryo (Bronchain et al., 2021). Apart from our article, this gene has yet never been mentioned so far in all published data relative to sea urchin development and it has never been integrated in GRNs described in this species. This was surprising given that the PSEN protein, which is part of the γ -secretase complex, is well known to have Notch as a substrate, which itself is well described in various species, including sea urchin, as controlling endoderm and gut development, differentiation of immune cells and even neurogenesis (Duggan and McCarthy, 2016; Oikawa and Walter, 2019; Otto et al., 2016). Our published data indicate that PSEN is first expressed in the whole early embryo, and becomes more and more confined during embryonic development until expression is restricted to the midgut, the hindgut, the primary mesenchyme cells (PMCs) and the secondary mesenchyme cells (SMCs) of the late gastrula (Bronchain et al., 2021). Transcription (WISH and RT-PCR) seems to mirror the expression of the protein until the gastrula stage, although our

results also suggest that the C- and N-terminal fragments of the PSEN protein, known to also be produced in many cell types and organisms including humans (Duggan and McCarthy, 2016), might play specific roles during sea urchin development. At the pluteus stage, we found that most cells expressing the PSEN protein are cilia cells located around the digestive system (Bronchain et al., 2021). We hypothesized that PSEN interact in the sea urchin embryo with the Hedgehog-Notch signaling pathway, which is known to influence neuronal specification in these cilia cells (Morris and Vacquier, 2019; Kong et al., 2015) and to regulate the development of the enteric nervous system in the gut (Liu and Ngan, 2014). By using a morpholino (MO)-based knockdown, we found that a critical level of PSEN is required at the cellular level for correct mitotic divisions and during development to reach blastula and then gastrula stages (Bronchain et al., 2021).

We were keen to test how the expression level of PSEN changes in embryos treated with LiCl, which has been used in diverse studies for tens of years to direct the development of the sea urchin and analyze the expression of various sea urchin genes. LiCl binds to glycogen synthase kinase-3 β and then acts as a vegetalizing agent by inducing an increase in the endoderm territory, at the expense of the ectoderm, without altering the mesodermal territories (Vonica et al., 2000). Furthermore, LiCl also reduces the expression of the oral marker Nodal, thus affecting the setup of the oral-aboral axis of the embryo, which fits with the conversion of part of the ectoderm into endoderm (Poustka et al., 2007). Given that PSEN is mostly expressed in endomesodermic territories until the gastrula stage, we anticipated that its expression would be upregulated in embryos treated with LiCl, but unexpectedly, this was not the case. Measurements of *PSEN* transcription led us to hypothesize the existence of *PSEN* NATs in these embryos, which might control the expression of the PSEN protein. We then analyzed the sense and antisense expression of other genes, *Endo16* and *Wnt5*, on the one hand, and of *Hnf6* and *Gsc*, on the other hand, which are typically markers, respectively, of endo-mesodermic or ectodermic territories (Poustka et al., 2007). We found that expansion of endomesoderm with LiCl or of the ectoderm with Zn²⁺ (Poustka et al., 2007) triggers changes in the sense and antisense transcription levels of all of these genes. We discuss that natural antisense transcription could, crucially, control the early development of the sea urchin.

RESULTS

Expansion of endomesodermic territories does not stimulate the synthesis of the PSEN protein

We started to investigate how expression of the PSEN protein changes in embryos treated with LiCl by performing immunostaining with an anti-N-terminal PSEN antibody (NterPSEN Ab). As we previously reported (Bronchain et al., 2021), control embryos express the PSEN protein at a higher level in the vegetal side at the gastrula stage (Fig. 1Aa). We therefore expected a similar strong fluorescence staining in LiCl-treated embryos, where endomesoderm is expanded at the expense of ectoderm. These embryos lack the archenteric invagination that occurs normally during gastrulation and eventually develop in exogastrulae as described by others (Poustka et al., 2007). However, and unexpectedly, the 24 h embryos treated with LiCl were uniformly and faintly fluorescent, the level of staining being markedly lower than that of the vegetal side of the control embryos (Fig. 1Ab). Similar results were obtained in embryos treated with 5 μ M U0126, an inhibitor of the MAPK cascade, which also leads to exogastrulation (Fig. 2Ac,c', 2Bc-c'; Fig. S1). Finally, we induced vegetalization by treating embryos with indirubin-3'-oxime (IO), which had been

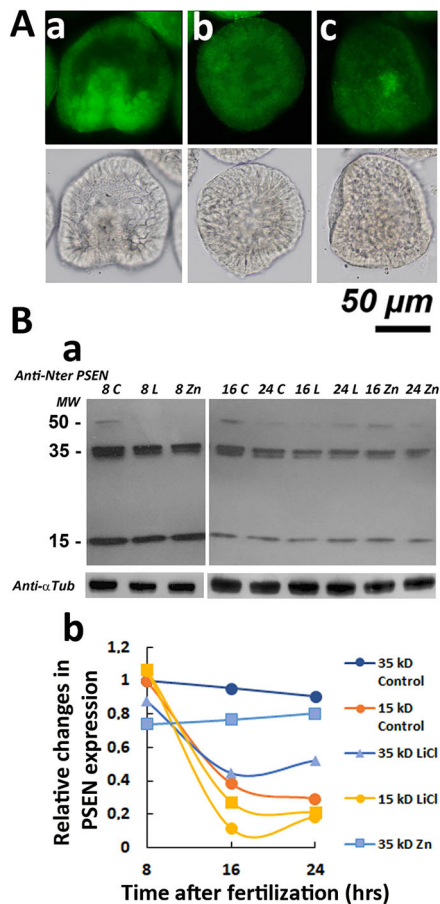


Fig. 1. Expression of the PSEN protein in vegetalized or animalized embryos. The same batch of 24-h-old embryos was used for immunofluorescence and (A) and western blotting (B). (A) Immunofluorescence labeling. Fluorescence images (upper panel) of embryos that were not treated (a, control), vegetalized with LiCl (b) or animalized with Zn^{2+} (c) were obtained after labeling with the anti-Nter PSEN Ab. Transmitted light images of the same embryos are shown in the lower panel. The control experiment with secondary antibody only did not give any signal (data not shown). The control gastrula is more heavily stained at the vegetal side, whereas a uniform and low staining is seen in LiCl- and Zn^{2+} -treated embryos. Images are representative of five experimental repeats. (B) Time course of PSEN expression during embryo development. C, control; L, LiCl treatment; Zn, Zn^{2+} treatment; number is number of hours. (a) A western blot was performed (a) using the same anti-Nter PSEN Ab as for immunofluorescence detection. Two major bands were detected (35 and 15 kDa), as previously reported (Bronchain et al., 2021), their intensity decreased after 8 h of development in control embryos (also see details in Bronchain et al., 2021). (b) Quantification of PSEN expression from the western blot analysis. The 35 kDa and the 15 kDa bands were quantified as explained in the Materials and Methods and expressed relative to the value determined in control 8 h embryos arbitrarily taken as 1. At each time, determinations in LiCl- and Zn^{2+} -treated embryos are lower than that of control embryos. Results are mean for three experimental repeats.

described to target GSK3 (Ribas et al., 2006). We first compared different bromoindirubins, 5BIO, 6BIO, 7BIO and IO in dose-response preliminary experiments in order to choose which was the best to induce vegetalization and at which concentration to use it (data not shown). 2 μ M IO induced a characteristic exogastrulation, and the embryos did not develop beyond the morula stage after treatment with either of the three other compounds, even when used at a lower concentration (data not shown). These embryos were as poorly stained as those treated with LiCl or U0126 (Fig. S1).

The above results suggest that the level of the PSEN protein expression is determined by mechanisms that occur during exogastrulation and not because of a non-specific effect of LiCl. We also performed the complementary experiment by treating embryos with zinc sulfate, which animalizes (anteriorizes) the embryos. These Zn^{2+} -treated embryos look like elongated blastula that never gastrulate, as reported by others (Poustka et al., 2007), and were also only faintly labeled for PSEN protein (Fig. 1Ac; Fig. S1). This result is expected given that these embryos have no or reduced endomesodermal cells and an expanded ectoderm (Poustka et al., 2007). Analysis by western blotting using the same anti-NterPSEN Ab corroborates these results, namely that there was a lower level of PSEN expression in LiCl- or Zn^{2+} -treated embryos than in control embryos (Fig. 1B).

WISH experiments suggest sense and antisense PSEN transcription

The surprising results described above on vegetalized embryos led us to evaluate transcription of the *PSEN* gene under the same conditions of embryonic development.

We first performed WISH experiments using a diaminobenzidine (DAB) staining protocol, similar to that we have previously reported (Bronchain et al., 2021). Usually, these tests are carried out on the basis that hybridization with the ‘sense’ probes are to serve as a control, i.e. a ‘calibration’ of the background noise. In other words, a set of treated or untreated embryos are hybridized with sense or antisense WISH probes under strictly the same conditions of buffers, hybridization time temperature, antibody concentrations and incubation and revelation time (see Materials and Methods), in order to improve the signal-over-noise ratio (to obtain the highest signal with the antisense probe together with the smallest possible signal with the sense probe). We performed our WISH tests following these recommendations. In all of our experiments, the color reaction was induced after incubation in an Nitro Blue Tetrazolium (NBT) and 5-bromo-4-chloro-3-indolyl phosphate (BCIP) (NBT/BCIP) solution over several hours (up to 26 h) and stopped at a time when a sufficiently strong and interpretable labeling appeared with the antisense *PSEN* probe in the control embryos, but without any signal with the sense *PSEN* probe. As expected, the antisense *PSEN* probe gave a strong staining around the blastopore, the midgut, the hindgut, the PMCs and the SMCs of the 24 h gastrula (Fig. 2Aa). An intense staining was obtained with the antisense *PSEN* probe in 24 h embryos treated with LiCl (Fig. 2Ab). This could be expected given that endomesoderm is expanded at the expense of ectoderm in these conditions. However, this increase in level of transcription after vegetalization observed by WISH, therefore, does not match that of PSEN protein expression, which decreases in these conditions as described above (Fig. 1A). Furthermore, although control embryos remained only poorly stained with the sense *PSEN* probe (Fig. 2Aa’), LiCl-treated embryos became strongly labeled with this probe (Fig. 2Ab’) after a 12-h incubation in the NBT/BCIP solution. Indeed, we observed that labeling of LiCl-treated embryos with the sense probe began after a 2-h incubation in the NBT/BCIP solution (data not shown). U0126- and IO-treated embryos gave the same results, that is a strong labeling with both the antisense (Fig. 2Ac and Fig. 2Ad, respectively) and the sense (Fig. 2Ac’ and Fig. 2Ad’, respectively) *PSEN* probes. It is therefore unlikely that the signal obtained with the sense *PSEN* probe is artifactual given that it is seen in embryos that have been vegetalized in three different ways and is not seen in untreated embryos. These results again reject the idea of a non-specific effect of LiCl as mentioned above.

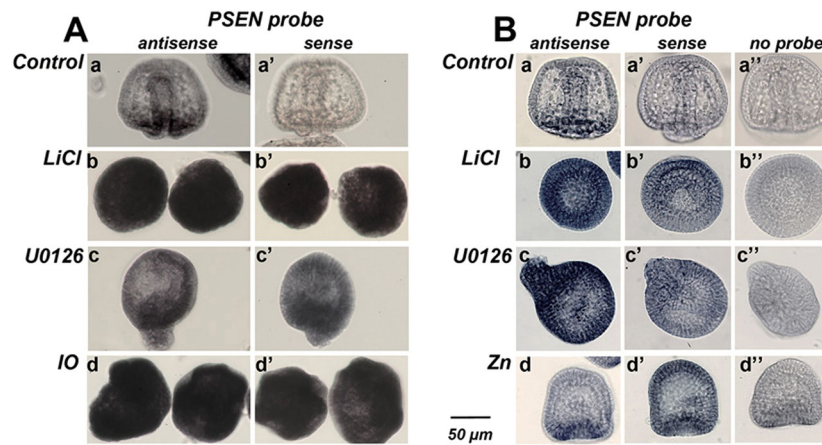


Fig. 2. *PSEN* transcript levels determined by WISH labeling in two different batches of embryos. A and B show two different batches of 24-h-old embryos. (A) Staining obtained with the *PSEN* antisense (a–d) and the sense (a'–d') probes are shown. Control gastrulae are strongly stained at the vegetal pole with the antisense probe (a) whereas no signal is detected with the sense probe (a'). Embryos treated with LiCl, U0126 or IO are uniformly and heavily stained with both probes (b–d and b'–d', respectively). (B) Images of embryos stained with the *PSEN* antisense (a–d) and the sense (a'–d') probes are compared to those of unstained embryos (a''–d''). Non-treated gastrulae (control) are stained at the vegetal pole with the antisense probe (a) but in that case show a weak signal with the sense probe (a'), which is detectable when compared to the image of non-labeled gastrula (a''). LiCl, U0126- and Zn²⁺-treated embryos are all uniformly and strongly stained with the *PSEN* antisense probe (b–d, respectively) while also showing a rather high labeling with the sense probe (b'–d', respectively) compared to that of the unstained embryos (a'–d'). Images are representative of five experimental repeats.

By repeating this experiment with other batches of embryos in order to also investigate the impact of Zn²⁺ treatment, we observed that the difference between the labeling intensities obtained with the sense and the antisense probes in the control embryos varies with the batch. Furthermore, in five out of nine batches, we could not obtain control embryos significantly labeled with the antisense probe without these embryos also becoming labeled with the sense probe. One such experiment is shown in Fig. 2B. The control embryos are only weakly labeled at the vegetative pole (Fig. 2Ba), the color reaction being stopped because embryos started to be more or less uniformly labeled with the sense *PSEN* probe (Fig. 2Ba'), when compared to the unlabeled embryos (Fig. 2Ba''). However, in this experiment, intense signals are still obtained with the antisense *PSEN* probe in embryos vegetalized with LiCl (Fig. 2Bb) or U0126 (Fig. 2Bc), or with the sense *PSEN* probe in both embryos (Fig. 2Bb',Bc'). Finally, in animalized embryos treated with Zn²⁺, the antisense (Fig. 2Bd) and the sense (Fig. 2Bd') *PSEN* probes gave a similarly high level of labeling.

These WISH experiments led us to hypothesize that the sense *PSEN* probe binds NATs that are contained in vegetalized or animalized embryos at a much higher level than in non-treated embryos of the same batch.

Natural antisense transcription of *PSEN* can be detected in embryos by strand specific RT-PCR and northern blotting

We used a strand-specific two-step RT-PCR approach to test whether antisense *PSEN* transcripts could be detected, keeping in mind that this method does not allow any quantification. As described in the Materials and Methods, a first step reverse transcriptase reaction (i.e. reverse transcription) was performed by using either a reverse- or a forward-specific *PSEN* primer in order to detect sense and antisense transcripts, respectively, which was followed by a PCR using two different pairs of primers designed from the *PSEN* mRNA (Table S1, Fig. S2). When using a reverse primer, amplicons corresponding to sense transcripts were detected at the expected size in 24 h embryos either untreated or treated with LiCl or Zn²⁺ (Fig. 3Aa). Similarly, amplicons of the same size

generated from antisense transcripts were also strongly detected after reverse transcription using a forward primer in LiCl- and Zn²⁺-treated embryos, the signal being faint in untreated embryos (Fig. 3Ab). Various negative controls were performed in order to exclude contamination by genomic DNA or by non-specific products, such as PCR without primers or one primer only or run after a reverse transcription performed without primers (see detailed protocols in Fig. S3). Furthermore, all primers used for these RT-PCR and qPCR described below were designed in different exons and on either side of an intron, thus limiting potential unwanted signal from contaminating genomic DNA.

We next analyzed total RNAs from 24 h embryos by northern hybridization (Fig. 3B). RNAs issued from five different batches of embryos were analyzed by using the same protocol. In all experiments, hybridization signals occurring at a size corresponding to ~1600 nucleotides were obtained with the antisense ³²P-*PSEN* probe, revealing sense transcripts, and were stronger in LiCl- and Zn²⁺-treated embryos compared to those obtained in untreated embryos (Fig. 3Ba). This size corresponds to that of the sea urchin *PSEN* mRNA found in *Paracentrotus lividus* (Bronchain et al., 2021) or in *S. purpuratus* (ID: SPU_006912, <https://www.echinobase.org/>). An additional RNA of ~3200 nucleotides was detected in three RNA preparations (Fig. 3Ba, Exp2) which, in this case, seemed to increase with Zn²⁺ treatment. We do not know the nature of this band. However, these results indicate that global expression of sense transcripts occurring in 24-h-old embryos increase after LiCl or Zn²⁺ treatment, which corroborates the *in situ* experiments. The sense ³²P-*PSEN* probe revealed a major antisense transcript of ~1600 nucleotides, a size corresponding to that of the *PSEN* mRNA, but which either did not change with the treatment (Fig. 3Bb, Exp1) or seemed to decrease in LiCl- and Zn²⁺-treated embryos (Fig. 3Bb, Exp1), depending on the RNA preparation. A second shorter RNA species (~700 nucleotides) was also detected, which was markedly more abundant in LiCl- and Zn²⁺-treated embryos in comparison with untreated embryos in the five RNA batches (Fig. 3Bb). Overall, these results suggest that NATs of different sizes are produced – NATs of comparable size to the *PSEN*

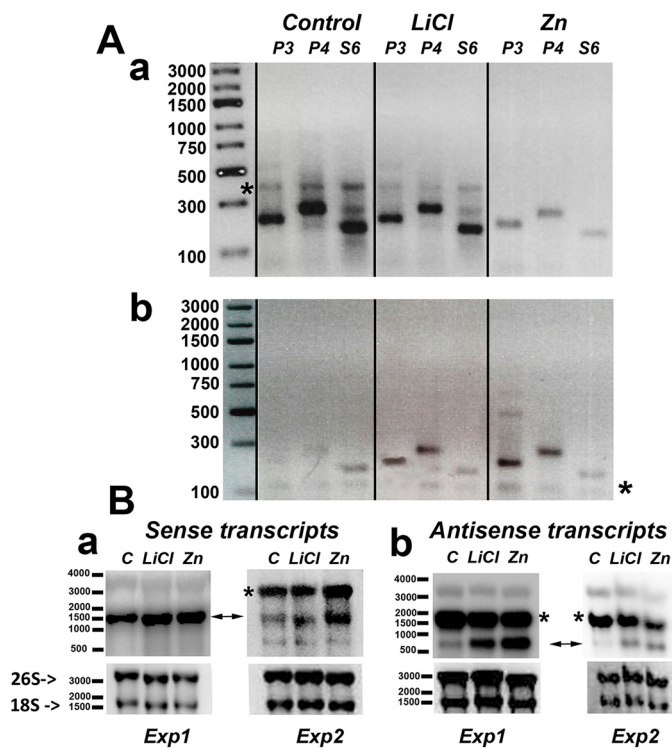


Fig. 3. Detection of *PSEN* sense and antisense transcripts by RT-PCR and northern blotting in 24 h embryos. (A) Semi-quantitative RT-PCR.

Two pairs of *PSEN* primers (P3 and P4) and S6 as an internal control have been used for PCR. (a) Detection of sense *PSEN* transcripts by amplifying cDNA generated by reverse transcription using the *PSEN* reverse primer (see Materials and Methods). PCR products of the expected size indicate that sense transcripts are expressed in untreated (control) and LiCl or Zn²⁺ treated embryos. A non-specific band is seen in all samples (*).

(b) Detection of antisense *PSEN* transcripts using the *PSEN* forward primer for reverse transcription and the same oligonucleotides for amplification. Similar amplicons are strongly detected in LiCl- and Zn²⁺-treated embryos but are only faintly visible in control embryos. A non-specific band is seen in all samples (*). Images are representative of six experimental repeats.

(B) Northern blots. 10 µg of total RNA extracted from two experiments (Exp1 and Exp2, representative of two and three batches of embryos, respectively) of 24 h embryos untreated (control, labeled 'C') or treated with LiCl or Zn²⁺ were run in parallel. (a) Sense transcripts. Hybridization was performed using the ³²P-*PSEN* antisense probe (upper panels). A band corresponding in size to that of the sea urchin *PSEN* mRNA (double arrow) was detected in all samples in both experiments. However, an additional signal (*) was detected in Exp2. (b) Antisense transcripts. Hybridization was performed using the ³²P-*PSEN* sense probe (upper panels). Two bands were detected, one with a size similar to that of the *PSEN* mRNA (*) and a smaller transcript (double arrow). As a loading control, the 26S and 18S rRNA bands were stained before transfer (lower panels). Variations in transcript levels are described in the main text.

sense transcription unit whose quantity varies or not according to the treatments, and NATs of smaller sizes whose quantity always increases with LiCl and Zn²⁺ treatment and could then cause the increased signal seen in WISH experiments.

WISH experiments suggest sense and antisense transcription of *Wnt5* and *Gsc*

An obvious question arose from the results described above: is antisense transcription also associated with the expression of genes others than *PSEN*? We then looked at the expression of two other genes, *Wnt5* and *Gsc* in WISH experiments by using the same protocol as that used for *PSEN*. *Wnt5* has been described to be

expressed first in endoderm and then in a patch of cells in the lateral border ectoderm after gastrulation (McIntyre et al., 2013). This pattern of expression was indeed seen after labeling of 24 h control embryos with the *Wnt5* antisense probe (Fig. 4Aa). *Gsc* is expressed in nearly all the oral ectoderm from blastula to pluteus stages (Croce et al., 2003), which fits with the faint signals obtained in control 24 h embryos with the *Gsc* antisense probe (Fig. 4Ba). However, despite several attempts to change times incubations and/or probe concentrations in our WISH protocol, we failed to get a sufficiently strong and interpretable signal with the antisense probes in all untreated embryos as reported by others for *Wnt5* (Ferkowicz and Raff, 2001; McIntyre et al., 2013) and *Gsc* (Angerer et al., 2001; Croce et al., 2003; Li et al., 2013; Saudemont et al., 2010) without also having one with the *Wnt5* (Fig. 4Aa') or the *Gsc* (Fig. 4Ba') sense probes (Fig. 4Ba'). A labeling with more or less strong intensity and which varies with the embryos was equally seen with the antisense and sense *Wnt5* probes in embryos treated with LiCl (Fig. 4Ab,b') or Zn²⁺ (Fig. 4Ac,c'). Although LiCl-treated embryos remained unlabeled with the antisense *Gsc* probe (Fig. 4Bb), they became, by contrast, strongly labeled with the sense *Gsc* probe (Fig. 4Bb'). A signal with variable intensity and which varies with the embryos was equally seen with the antisense (Fig. 4Bc) and sense (Fig. 4Bc') *Gsc* probes in Zn²⁺-treated embryos. Three other experiments gave similar results, all of them giving LiCl-treated embryos, which became very dark with the sense *Gsc* probe, whereas control embryos or LiCl-treated embryos remained only faintly labeled or even unlabeled with the antisense *Gsc* probe (data not shown).

Analysis by qPCR shows sense and antisense transcription corresponding to various genes of the endo-mesodermic or ectodermal territories

In order to reinforce the idea that NATs for *PSEN*, *Wnt5* and *Gsc* are expressed in sea urchin embryos, sense (S) and antisense (AS1 and AS2) transcription was measured by qPCR after strand-oriented reverse transcription performed with specific primers as described in the Materials and Methods (Table S1, Fig. S2), a strategy similar to that described above for RT-PCR. This also allowed us to extend this investigation to more genes and to quantify potential variations. We added *Endo16* and *Hnf6* to our study. *Endo16* is expressed in endoderm and has been studied in great detail (Sethi et al., 2009). The *Hnf6* gene encodes a member of the ONECUT family of transcription factors, which are required for the activation of some PMC differentiation genes (Otim et al., 2004). It also plays a role after gastrulation in the oral ectoderm GRN and in the neurogenic ciliated band formation. As indicated above for RT-PCR experiments, control experiments were run after reverse transcription performed either with RNA extracts without primers, or with primers but without RNA, all giving no signal (Table S2). Both sense and antisense transcripts that are detected have been sequenced and indeed correspond to each analyzed gene, *PSEN*, *Gsc*, *Wnt5*, *Hnf6* and *Endo16* (Fig. S4, Table S4). As expected, the sense transcription of the two endomesodermic genes, *Endo16* and *Wnt5*, increased in LiCl-treated embryos (Fig. 5Aa) and decreased in Zn²⁺-treated embryos (Fig. 5Ba). By contrast, and also as expected, the sense transcription of the two ectodermic genes, *Hnf6* and *Gsc* substantially decreased (Fig. 5Aa) and increased (Fig. 5Ba) in three batches of embryos treated with LiCl and Zn²⁺, respectively. Sense transcription of *PSEN* clearly increased in all batches of embryos that were either vegetalized (Fig. 5Aa) or animalized (Fig. 5Ba). This corroborates results obtained in the WISH experiments described above. Importantly, antisense transcription was clearly detected for each treatment, and similar results were

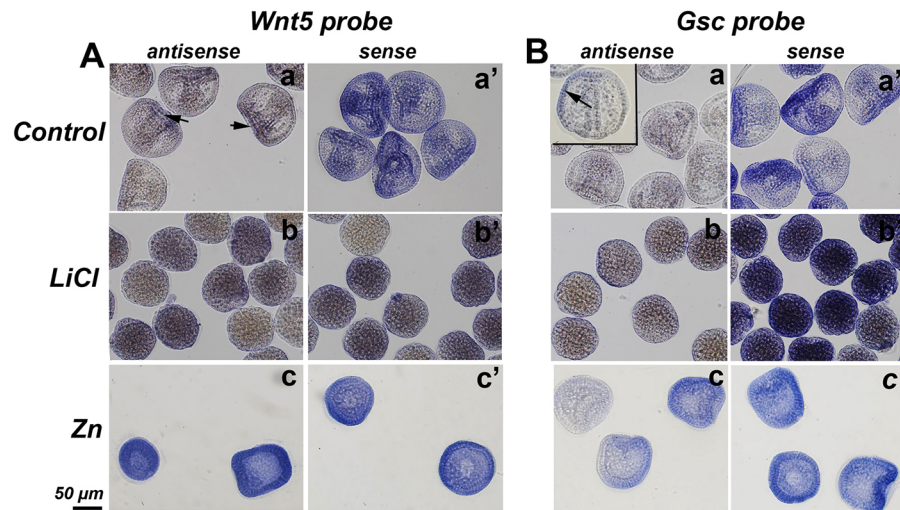


Fig. 4. Detection of *Wnt5* and *Gsc* antisense transcripts by WISH. 24 h embryos non-treated (control) or treated with LiCl or Zn^{2+} are labeled with antisense probes to detect sense transcripts (a–c) or sense probes to detect antisense transcripts (a'–c'). (A) Transcription of *Wnt5*. Sense transcripts (left panel) are expressed in the vegetal pole (arrow) of the control embryos (a) and uniformly in embryos treated with LiCl (b) or Zn^{2+} (c) where the intensity of the signal varies between embryos. Antisense transcripts (right panels) are expressed uniformly in all embryos (a'–c') with an intensity that also clearly varies between embryos after in LiCl treatment (b'). (B) Transcription of *Gsc*. Expression of sense transcripts (left panel) is barely detected in the oral ectoderm (arrow, image is presented at 1.5× main image) of control embryos (a), remains low in LiCl embryos (b) and varies between embryos in Zn^{2+} embryos (c). A uniform expression of antisense transcripts (right panels) varies between control embryos (a'), is very intense in LiCl embryos (b') and substantially higher in Zn^{2+} embryos. Images are representative of three experimental repeats.

obtained in the two sets of measures AS1 and AS2 (Fig. 5Ab versus Fig. 5Ac and Fig. 5Bb versus Fig. 5Bc). For *Endo16*, *Wnt5* and *PSEN*, antisense transcription predominantly followed the same variations as sense transcription, that is, it increased and decreased in embryos treated with LiCl (Fig. 5Ab,c) and Zn^{2+} (Fig. 5Bb,c), respectively. These results support the idea of an increase in *PSEN* antisense transcription after LiCl and Zn^{2+} treatment, as suggested above and also fit with the positive staining of embryos with the WISH sense *Wnt5* probe (Fig. 4Ab'). Results appear more variable in the case of *Hnf6* and *Gsc*, increase or decrease in AS1 or AS2 expression being measured in embryos treated with either LiCl (Fig. 5Ab,c) or Zn^{2+} (Fig. 5Bb,c).

We then calculated the ratio of antisense to sense transcription (AS1/S and AS2/S) for each gene (Fig. 6). In control embryos, AS1/S (Fig. 6Aa) and AS2/S (Fig. 6Ba) ratios calculated for *Hnf6*, *Wnt5* and *PSEN* varied from ~10 to ~20, whereas the ratios exceeded 50 for *Endo16* and *Gsc*. LiCl treatment did not notably change these ratios for *Hnf6*, *Wnt5* and *PSEN*, but increased them significantly for *Endo16* (Fig. 6Ab) and *Gsc* (Fig. 6Bb). It must be noted that seven out of eight values of the *Gsc* AS2/S ratio exceeded 100, which means that in this instance there are more antisense transcripts than sense transcripts. This might explain why the WISH staining with the *Gsc* sense probe is particularly strong in LiCl embryos (Fig. 4Bb').

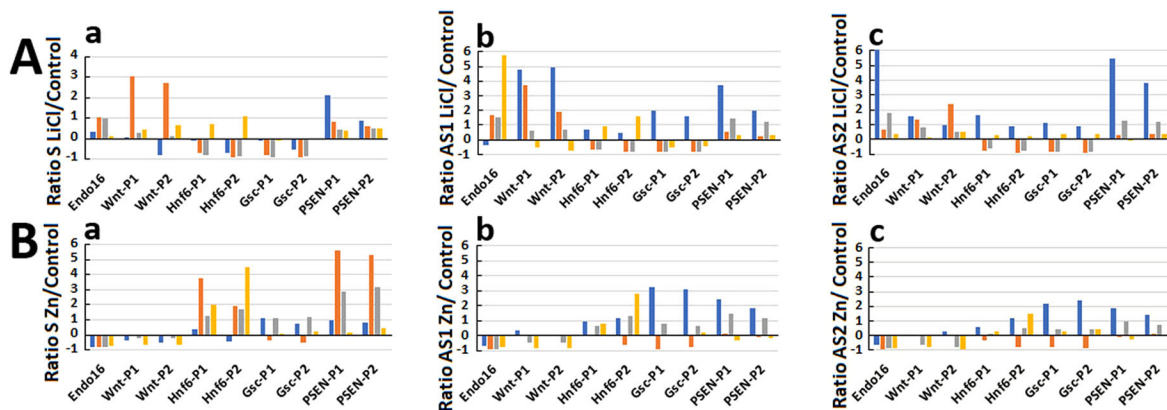


Fig. 5. Effect of LiCl and Zn^{2+} treatment on the levels of *Endo16*, *Wnt5*, *Hnf6*, *Gsc* and *PSEN* sense and antisense transcripts. RT-qPCR results from four batches of embryos (Exp1–Exp4) are shown in different colors. qPCR was performed by using one pair of primers for *Endo16* and two different pairs of primers (P1 and P2) for *Hnf6*, *Wnt5*, *Gsc* and *PSEN* (see Materials and Methods). Results are compared to those from non-treated embryos of the same batch and given as $R_{GOI} - R_{S18}$ where R is calculated following the formula: $R = E_{GOI}^{(Cq \text{ control} - Cq \text{ experiment})} / E_{S18}^{(Cq \text{ control} - Cq)}$ for sense (S) and antisense (AS1 and AS2). Negative and positive values thus indicate a decrease or an increase in transcription compared to control, respectively. (A) Effect of LiCl. (a) Sense transcription. qPCR was performed on cDNAs obtained with a combination of reverse primers (S-RT) as described in the Materials and Methods. (b,c) Antisense transcription. cDNAs were obtained with a combination of forward primers, RT-F1 (b) or RT-F2 (c) as described in the Materials and Methods. (B) Effect of Zn^{2+} . qPCR was performed on cDNAs as described above for LiCl. (a) Sense transcription. (b,c) Antisense transcription.

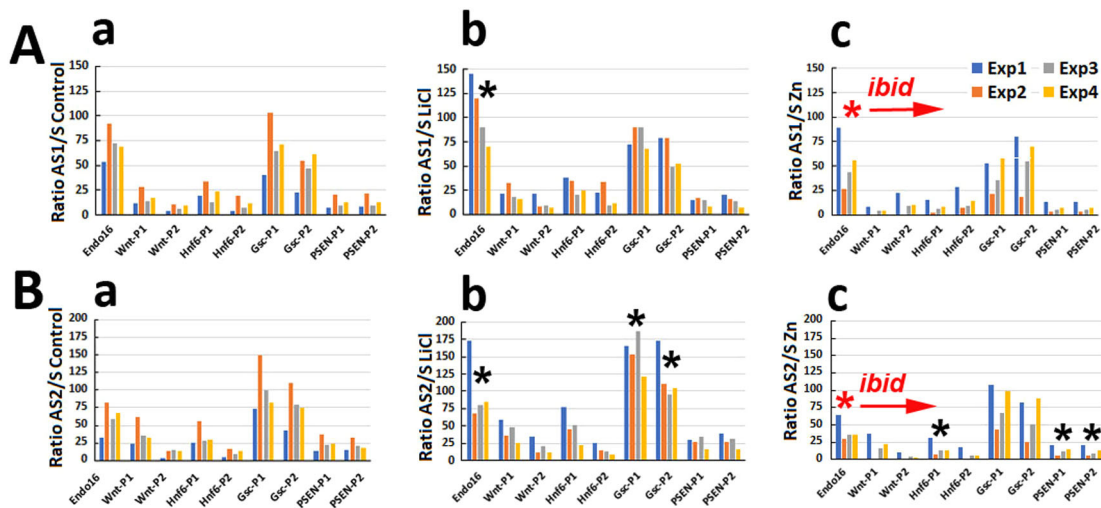


Fig. 6. Modification of the *Endo16*, *Wnt5*, *Hnf6*, *Gsc* and *PSEN* antisense-to-sense transcript ratio upon LiCl and Zn^{2+} treatment. All ratios have been calculated as $[(E_{GOI}^{-ct}/E_{S18}^{-ct}) AS/(E_{GOI}^{-ct}/E_{S18}^{-ct}) S] \times 100$ in control (a), LiCl (b) and Zn^{2+} (c) treated embryos. (A) Ratios AS1/S. (B) Ratios AS2/S. Means \pm s.e.m. of the four batches of embryos have been calculated for each gene and ratio. A few values (highlighted with a black star) obtained in LiCl- or Zn^{2+} -treated embryos are significantly different (Student's *t*-test, $P < 0.05$) from those obtained in controls. Values obtained in Zn^{2+} -treated embryos are all (red star, *ibid*) significantly lower (two-tailed *t*-test, $P < 0.05$) than those measured in LiCl.

The means of the four values determined for each gene and ratio indicate that AS1/S and AS2/S ratios have a general tendency to increase in LiCl-treated embryos (Fig. 6Ab versus Fig. 6Aa and 6Bb versus Fig. 6Ba, respectively) and to decrease in Zn^{2+} -treated embryos (Fig. 6Ac versus Fig. 6Aa and 6Bc versus Fig. 6Ba) when compared to those measured in untreated controls. However, the ratios AS1/S for *Endo16* (Fig. 6Ab), AS2/S for *Endo16* and *gsc* (Fig. 6Bb) in LiCl-treated embryos and AS2/S for *Hnf6* and *PSEN* in Zn^{2+} -treated embryos (Fig. 6Bc) are the only ones to be statistically different from those measured in control embryos. Nevertheless, all ratios AS1/S and AS2/S calculated in Zn^{2+} -treated embryos are statistically lower than those measured in LiCl-treated embryos (Fig. 6Ac versus Fig. 6Ab and Fig. 6Bc versus Fig. 6Bb). In conclusion, the orientation of embryonic development might change the antisense to sense transcription ratio for a given gene in one direction or another.

DISCUSSION

Here we show, for a number of genes, that antisense transcription occurs in the sea urchin embryo to levels that need to be taken into account when quantifying developmentally regulated gene expression. Our results also indicate that the antisense to sense transcription ratios differ between genes during normal development. This could provide new insights into the control of gene expression in a specific tissue during normal development. In addition, significant changes in sense to antisense transcript levels occur after treatment with LiCl or Zn^{2+} , agents that have been used for decades as ‘manipulators’ of GRNs (Poustka et al., 2007). Li^+ exerts a myriad of physiological and biochemical effects, by acting directly or indirectly on targets such as GSK3, which is part of the Wnt/ β -catenin pathway, which is crucial for the anterior-posterior axis establishment (Jakobsson et al., 2017), or by binding to a variety of DNA motifs and transcription factors (Roux and Dosseto, 2017). Similarly, Zn^{2+} is the cofactor in ~3000 zinc metalloproteins, thus impacting a variety of Ca^{2+} , redox and phosphorylation pathways (Maret, 2017; Kręzel and Maret, 2016). It is therefore impractical to determine how Li^+ and Zn^{2+} act to activate and inhibit, respectively, the antisense transcription.

The detection of antisense transcription in the sea urchin – could it be a measurement artifact?

We are confident that antisense transcription is not a measurement artifact. First of all, it would be expected that any non-specific hybridization to transcripts during WISH or qPCR in LiCl- or Zn^{2+} -treated embryos would also occur in control embryos. Different batches of embryos give mostly similar results for each gene in each type of experimentation. Furthermore, an increase in an antisense signal after Li or Zn^{2+} treatment was obtained by three different methods, WISH, RT-PCR and qPCR, using a variety of specific oligonucleotide probes.

Concerning WISH and northern blotting experiments, we do not know whether other authors detected any signal with sense probes as they have either not been used for *Gsc* (Angerer et al., 2001; Li et al., 2013) and *Wnt5* (McIntyre et al., 2013), or they were used but the results were not shown for *Gsc* (Saudemont et al., 2010; Croce et al., 2003) or *Wnt5* (Ferkowicz and Raff, 2001). It is possible that sense RNA probes could bind a nonspecific target or genomic DNA remnants, which would not be removed after treatment of the samples with DNase. However, it is unlikely that such a background or any other nonspecific signal detected by sense probes would increase after LiCl or Zn^{2+} treatment.

Another question concerns the level of staining in control embryos with the sense *Wnt5* and *Gsc* WISH probes, which is higher than that obtained with the corresponding antisense probes (Fig. 4) (although the level of sense transcripts is higher than those for the antisense transcripts as measured by qPCR). However, WISH is not strictly speaking a quantitative method, and it is difficult to compare expression levels measured by this technique with qPCR. It is also unlikely that the efficiency of the antisense probe interaction for the sense transcript differs from that of the sense probe interaction for the antisense transcript. An explanation might be that antisense transcripts differ from sense mRNA by adopting different 2D or 3D structures or by having different binding to proteins etc., which would render them more reactive to the WISH probes than the sense transcripts (Yilmaz and Noguera, 2004). Nevertheless, this does not detract from the fact that antisense transcription can indeed be detected.

What about our RT-PCR and qPCR experiments?

Firstly, all controls we can think of have been performed and gave no signal, as RT-PCR or qPCR was performed with intron spanning primers on cDNA made after reverse transcription without primer or on the starting RNA preparation, or performed with one primer only. This rules out amplification of contaminant genomic DNA or of another RNA target.

Secondly, if measurements are attributable to noise, the ratio of AS/S for a given gene would not change after treatment with LiCl or Zn²⁺, which is not always the case as measured for *Endo16*, *Gsc* and *PSEN*. Moreover, values of ratios AS1/S and AS2/S are significantly lower for all genes in Zn²⁺-treated embryos when compared to those measured in LiCl-treated embryos.

Thirdly, all sense and antisense transcripts that are detected have been sequenced and correspond to each analyzed gene (*PSEN*, *Gsc*, *Wnt5*, *Hnf6* and *Endo16*).

Making sense of antisense transcription in the sea urchin embryo

Natural antisense transcription has been reported in many animal models (Dahary et al., 2005), from *Drosophila* (Camilleri-Robles et al., 2022) to crustaceans (Zeng et al., 2018) and mollusks (Hongkuan et al., 2021) to humans (Mukherjee et al., 2021). Roles of microRNAs (Song et al., 2012; Remsburg et al., 2019) and Piwi-interacting RNA (piRNA) (Yajima et al., 2014) have been described in sea urchin development, but to our knowledge this is the first reporting of natural antisense transcription corresponding to coding genes in this species. A review by Ransick (2004) states that “although it is common to use the antisense RNA as a control for background, the level of noise is highly variable among different control probes”. ‘Noise’ might then be antisense transcription, which would lead to a variability of gene expression levels (Liu et al., 2017) and which particularly relates to the synthesis of lncRNA (Nojima and Proudfoot, 2022). We do not know the size of the NATs that we detect here. WISH probes have been made so as to correspond to the full size coding (CDS) sequence of each gene and can therefore bind any part of the corresponding RNA. In northern blotting experiments, one *PSEN* antisense transcript of ~600 bp and one corresponding to the full-size transcript are the only forms detected. Although antisense transcripts can be transcribed through the action of a promoter, similar to that of a protein-coding gene, they can also be made from repetitive sequences, such as ALU or SINE, and even be produced from the introns of genes. A band that has the same size than that of the sense one might then correspond to the full-length transcript but this size may be fortuitous and could well correspond to an antisense transcript that contains intron(s), or part of 3' or 5' UTR. It would potentially be interesting to use more sensitive methods, such as a hybridization chain reaction (HCR), to follow the expression of these NATs during the sea urchin development (Choi et al., 2016).

It is estimated today that up to 40% of the human transcriptome is transcribed in an antisense manner (Mukherjee et al., 2021). In zebrafish, ~50% of lncRNAs are transcribed during development in an antisense direction to a protein-coding gene (reviewed in Pillay et al., 2021). These lncRNAs are specifically enriched in early-stage embryos, with several of them showing tissue-specific expression and distinct subcellular localization patterns, and being associated with specific pathways and functions ranging from cell cycle regulation to morphogenesis (Pauli et al., 2012). The antisense-to-sense transcription level ratios, to our knowledge, have not been determined in all these studies, which, however, help explain those we report here. It would be interesting to perform a

similar analysis in the sea urchin and investigate its whole transcriptome by using appropriate bioinformatic pipelines (Krappinger et al., 2021).

Is there an antisense-to-sense transcript ratio that is adjusted for each gene in order to define orientation of development?

Our qPCR measurements indicate that antisense-to-sense transcript ratios have a tendency to increase in LiCl-treated embryos and to decrease in those treated with Zn²⁺ embryos, with all ratios calculated in Zn²⁺-treated embryos being significantly lower than those measured in LiCl-treated embryos. An intriguing question concerns the very high AS/S ratios observed for *Gsc* and *Endo16*, even in control embryos. This ratio AS/S for *Gsc*, which exceeds 100 in LiCl-treated embryos, means that there are more antisense than sense *Gsc* transcripts in these embryos. This might explain the very strong signal in WISH staining experiments with the sense *Gsc* probe although the level of AS transcripts decreases after Li treatment. *Gsc* belongs to the family of homeobox genes (Howard-Ashby et al., 2006) and antisense transcription could be one of their particularities. As a matter of fact, some of these genes are known to be controlled by lncRNAs in mice and in humans, but these lncRNAs are expressed upstream of the genes that they regulate and do not correspond to the antisense coding frame of these genes (Casaca et al., 2018). Another hypothesis is that antisense transcription is driven through the TATA box of the *Gsc* gene (Koster and Timmers, 2015). This could represent a novel mechanism to explain mesendoderm specification as hypothesized in human embryonic stem cells, where the TATA box-binding protein-related factor 3 interacts with the TATA box of key mesendodermal genes including brachyury (*TBXT*) and *GSC* (Liang et al., 2020). Concerning *Endo16*, antisense transcription could control the expression of the two alternative spliced *Endo16* transcripts that are produced during gastrulation and which have distinct temporal as well as spatial expression patterns (Godin et al., 1996). It is necessary to analyze whether a high ratio for antisense-to-sense transcripts can be identified for other genes known to be alternatively transcribed during development.

The NATs that we detect here correspond, at least in part, to the coding sequence of genes and can therefore interact with the corresponding sense transcript, which could directly affect transcription and protein translation (Zhao et al., 2020). This interaction between sense and antisense would also lead to the formation of double-stranded RNA (dsRNA) (Sadeq et al., 2021; Chen and Hur, 2022). dsRNA had indeed been detected in sea urchin embryos 50 years ago (Kronenberg and Humphreys, 1972), but there has been no other reported detection since then. dsRNAs have been suggested to serve as a cellular signaling molecule to coordinate normal physiological processes (Sadeq et al., 2021). For all these reasons, NATs might consequently play a major role during development. Sense transcripts naturally form dsRNA structures, mostly from repetitive sequences within them (Sadeq et al., 2021). One can wonder whether such secondary double-stranded structures, possibly formed in the *Gsc* or *Wnt5* sense transcripts (Gruber et al., 2008 and <http://rna.tbi.univie.ac.at/>), could be detected by WISH with the sense probe. However, we believe this is unlikely given that modifications in the antisense WISH signal would follow that of the sense transcript level if this were the case. However, this does not occur, in particular in LiCl-treated embryos, which give a strong WISH signal with the sense *Gsc* probe, whereas the level of sense transcripts decreases compared to that of untreated embryos.

Different mechanisms for synthesis of antisense transcripts have been described in the literature (Zhao et al., 2020). Although they certainly can be transcribed through the action of a promoter, similar to that of a protein-coding gene, they can also be transcribed from repetitive sequences such as ALU or SINE and even be transcribed from the introns of genes. Antisense transcription could also originate from a gene transcribed nearby or even overlapping the opposite strand of the genes analyzed here. The latter is unlikely since no gene is transcribed on the opposite strand of each gene studied here (as seen in <https://www.echinobase.org/>). The sea urchin might be a valuable model for such a study, and new performant approaches to generate and process genomic and transcriptome resources have recently been used to study the genome in this model (Arenas-Mena et al., 2021; Marlétaz et al., 2023). Another potentially interesting point for research is the fact that there is no RNA reverse transcriptase in eukaryotes except the telomerase, which can have this activity (Smith et al., 2020). This enzyme is sensitive to Zn^{2+} , and the decrease in AS transcription after Zn^{2+} treatment might suggest such a mechanism. Could there be an antisense or sense gradient in the same way that there is a gradient of the Wnt/GSK3 pathway from the vegetative pole to the animal pole of the embryo? Finally, the human *PSEN1* and *PSEN2* play a role in Alzheimer's disease (AD) and a few antisense transcripts of these genes have indeed been reported (Zucchelli et al., 2019), but their role has never been investigated. We hope that our work will open the door to new horizons, in the field of developmental biology and in that of AD.

MATERIALS AND METHODS

Handling of gametes and preparations of samples for western blotting, immunostaining, WISH and RT-PCR or qPCR analysis

Collection of gametes, fertilization and development of embryos, as well as preparations of dry pellets for western blotting and of fixed embryos for immunostaining and WISH were performed as described previously (Bronchain et al., 2021). Embryos were developed in artificial sea water (ASW, Reef Crystals Instant Ocean). Either 30 mM LiCl (Sigma-Aldrich), 5 μ M U0126 (Promega) or 2 μ M IO to induce vegetalization or 300 μ M zinc sulfate (Sigma-Aldrich) to induce animalization were added to the embryo culture at the four cell stage.

Western blot analysis and immunostaining

Protocols have been described in our previous article (Bronchain et al., 2021). Western blotting was performed by using an anti-NterPSEN Ab, made in rabbit immunized against a peptide located in the Nter part of the *Paracentrotus lividus* PSEN sequence (see Bronchain et al., 2021 for details) and an anti- α tubulin mouse Ab (#CP06, Calbiochem).

PSEN immunostaining was performed by using the same anti-NterPSEN Ab associated with an anti-rabbit-IgG FITC-conjugated secondary antibody (Jackson ImmunoResearch).

WISH and northern blotting probes

PSEN sense and antisense probes were obtained as described in our previous article (Bronchain et al., 2021). *Wnt5* and *Gsc* clones were gifts from J. Croce (Laboratoire de Biologie du Développement de Villefranche-sur-Mer, France; Croce et al., 2003; McIntyre et al., 2013). The *Gsc* insert was initially cloned in pBluescript II KS⁺ while the *Wnt5* insert, initially cloned in pCS2⁺, was transferred to pBluescript II KS⁺ (sequences are given in Table S3). For both methods, sense (to detect antisense RNA) and antisense probes (to detect sense RNA) were synthesized as described in our previous article (Bronchain et al., 2021) by using Hind III/T7 RNA polymerase and BamH1 / T3 RNA polymerase, respectively. Probes were labeled using digoxigenin-11-UTP (Roche) for WISH experiments or with α P³²UTP for Northern Blot experiments.

WISH

A DAB staining protocol was applied on fixed embryos by using buffers and conditions of hybridization time and temperature as described by Duboc et al. (2004).

Preliminary tests were carried out for each gene (*PSEN*, *Gsc* and *Wnt5*) to determine the antibody concentrations, incubation and revelation times that give the 'best signal' (i.e. the highest signal with the antisense probe together with absence of signal with the sense probe). This led us to use each RNA probe at a 1:100 dilution (0.05 ng/ μ l) and to apply a 2 h. incubation with a 1:5000 dilution of anti-digoxigenin antibody (Roche, ref 11093274910) in all experiments. However, as described in the text, different incubation times in the NBT/BCIP solution were used (up to 26 h) according to the gene studied.

Northern blotting

Total RNA was purified from dry pellets of embryos with a RNeasy Plus Micro Kit (Qiagen) following the manufacturer's protocol. Sample quantity and purity were estimated by measuring the ratios of spectrophotometric absorbance at 260/280 nm and 260/230 nm. RNA was stored at -80°C before use.

10 μ g RNA were run on 2% agarose-formaldehyde gels and then transferred overnight to Hybond N membranes (Amersham). A 3 h prehybridization was performed in 50% formamide, 5 \times Denhardt's, 5 \times SSPE, 0.5% SDS and 100 μ g/ml denatured salmon sperm DNA (Thermo Fisher Scientific). Hybridization was carried out for 40 h at 57 $^{\circ}\text{C}$ in the same buffer containing the labeled probes. Blots were washed two times for 5 min in 6 \times SSPE, 0.5% SDS at room temperature, one time for 45 min in 1 \times SSPE, 0.1% SDS at 37 $^{\circ}\text{C}$, and one time for 45 min in 1 \times SSPE, 0.1% SDS at 50 $^{\circ}\text{C}$. They were finally analyzed using a Typhoon phosphor imager (GE) after a 24 h exposure.

Semi-quantitative RT-PCR and qPCR

The same total RNA preparations were used for northern blotting (described above), RT-PCR and qPCR.

Sequences of all primers and their relative positions on each gene are listed in Table S1 and Fig. S2, respectively. Ability to make self-dimers or cross primer dimers have been tested (<https://www.premierbiosoft.com/netprimer/> or <https://www.thermofisher.com/fr/fr/home/brands/thermo-scientific/molecular-biology/molecular-biology-learning-center/molecular-biology-resource-library/thermo-scientific-web-tools/multiple-primer-analyzer.html>) for all dimers, pairs of primers used for qPCR and mix of primers used for sense and antisense reverse transcription.

Detection of *PSEN* transcripts by RT-PCR was performed as described in our previous report (Bronchain et al., 2021). We used the SuperScript IV RT-kit (Invitrogen) for reverse transcription. cDNAs corresponding to sense transcripts were obtained from 1 μ g RNA with a mixture of reverse primers corresponding to *PSEN* and *S6* (S2-RT, Table S1). cDNAs corresponding to antisense transcripts were obtained with a mixture of forward primers corresponding to *PSEN* and the same *S6* reverse primer (F3-RT, Table S1).

PCR was then performed as described previously (Bronchain et al., 2021) with two different pairs of *PSEN* primers (PSEN-P3 and PSEN-P4) and with *S6* primers (*S6*-P) (Table S1). Aliquots (10–50%) of each amplicon were run on 2% agarose gels.

For qPCR, RNA quality and integrity were further analyzed by capillary electrophoresis (Fragment Analyzer, Agilent Technologies) to determine the RNA quality number (RQN) for each sample. Defined on a scale ranging from 1 to 10, the mean RQN of all samples was 9.9, indicating very good RNA quality. qPCR was run on samples of cDNAs that were obtained as followed. We also used the SuperScript IV RT-kit (Invitrogen) for reverse transcription. cDNAs corresponding to sense transcripts were obtained with a mixture of reverse primers corresponding to *PSEN*, *Wnt5*, *Gsc*, *Endo16*, *Hnf6* and *S18* (S-RT, Table S1). cDNAs corresponding to antisense transcripts were obtained with two different mixtures (F1-RT and F2-RT, Table S1) containing forward primers corresponding to *PSEN*, *Wnt5*, *Gsc*, *Endo16* and *Hnf6* with the *S18* reverse primer *S18*-Rv3.

High-throughput qPCR was performed using the high-throughput platform BioMark™ HD System and the FlexSix GE Dynamic Arrays

(Fluidigm®). The 12 pairs of primers (Table S1) were first tested in multiplexing condition with the CFX method. Melt curve analysis confirmed the specificity of each pair of primers to detect only one gene after multiplexed pre-amplification. Specific target pre-amplification was performed as follows: each diluted cDNA was used for multiplex pre-amplification in a total volume of 5 µl containing 1 µl of 5× Fluidigm® PreAmp Master Mix, 1.25 µl of cDNA, 1.25 µl of pooled assay with an original concentration of each assay of 10 µM and 1.5 µl of nuclease-free water. The cDNA sample was subjected to pre-amplification following the temperature protocol: 95°C for 2 min, followed by 14 cycles at 95°C for 15 s and 60°C for 4 min. The pre-amplified cDNAs was diluted 5× by adding 20 µl of low TE buffer and stored at -20°C before qPCR.

The expression of 12 target genes was quantified in 72 samples by qPCR on seven 12.12 partition microfluidic chips (Biomark-HDTM, Fluidigm). One 12.12 partition contained one sample replicate of each partition, a non-template control (NTC), and a serial dilution of cDNA samples used as a standard curve to calculate the primer efficiencies. 4 µl of Sample Master Mix (SMM) consisted of 1.8 µl of 5× diluted pre-amplified cDNA, 0.2 µl of 20X Sample Loading Reagent (Fluidigm®), 0.2 µl of 20X Binding dye buffer (Fluidigm®), 0.2 µl of 20× EvaGreen™ (Biotium®) and 1.6 µl of 2× Gene Expression PCR Master Mix (Life Technologies, Thermo Fisher Scientific). Each 4 µl Master Mix Assay (MMA) consisted of 2 µl assay 20× and 2 µl of 2× assay loading reagent (Fluidigm®). 3 µl of each SMM and each MMA premixes were added to the dedicated wells. The samples and assays were mixed inside the chip using HX IFC controller (Fluidigm®). The loaded Dynamic Array was transferred to the Biomark™ real-time PCR instrument and subjected to PCR experiment [50°C (10 min), 95°C (10 min), 95°C (15 s), 60°C (1 min)] for 40 cycles followed by melting curve analysis (1°C every 3 s). The parameters of the thermocycler were set with ROX as passive reference and single probe EvaGreen as fluorescent detector. To determine the quantification cycle C_q, data were processed by automatic threshold for each assay, with linear derivative baseline correction using BioMark Real-Time PCR Analysis Software 4.5.2 (Fluidigm®). The quality threshold was set at the default setting of 0.65.

Relative quantification of each gene expression level was normalized according to gene expression of *SI8*, which was stable throughout the experiments. It was generated using Pfaffl's method, which considers the efficiencies of the primers (Pfaffl, 2001). Fold change between experimental and control groups was calculated for each sample as the difference of C_q between reference genes and the gene of interest (GOI) in control and experimental conditions following the formula: $R = E_{GOI}^{(Cq_{control} - Cq_{experiment})} / E_{ref\ gene}^{(Cq_{control} - Cq_{experiment})}$. qPCR performed as control experiments on products of reverse transcriptase obtained with RNA without primer or primers without RNA gave no signal.

Acknowledgements

We thank C. Billam for correcting our manuscript.

Competing interests

The authors declare no competing or financial interests.

Author contributions

Conceptualization: O.B., H.P., B.C.; Methodology: O.B., B.D., M.D., H.P., S.L., L.P.-C., B.C.; Validation: O.B., B.D., B.C.; Formal analysis: O.B., B.D., M.D., H.P., S.L., L.P.-C., K.S., B.C.; Investigation: O.B., B.D., H.P., S.L., B.C.; Resources: O.B., B.C.; Data curation: B.D., B.C.; Writing - original draft: B.C.; Writing - review & editing: O.B., B.C.; Visualization: O.B., B.C.; Supervision: B.C.

Funding

This research was supported by the Centre National de la Recherche Scientifique (CNRS: UMR 9197), Université Sorbonne Paris Cité and Université Paris-Saclay, and LABEX Dynamo ANR-11-LABX-0011-01.

Data availability

All relevant data can be found within the article and its supplementary information.

References

Angerer, L. M., Oleksyn, D. W., Levine, A. M., Li, X., Klein, W. H. and Angerer, R. C. (2001). Sea urchin goosecoid function links fate specification along the animal-vegetal and oral-aboral embryonic axes. *Development* **128**, 4393-4404. doi:10.1242/dev.128.22.4393

- Arenas-Mena, C., Miljovska, S., Rice, E. J., Gurses, J., Shashikant, T., Wang, Z., Ercan, S. and Danko, C. G. (2021). Identification and prediction of developmental enhancers in sea urchin embryos. *BMC Genomics* **22**, 751. doi:10.1186/s12864-021-07936-0
- Bronchain, O., Philippe-Caraty, L., Anquetil, V. and Ciapa, B. (2021). Precise regulation of presenilin expression is required for sea urchin early development. *J. Cell Sci.* **134**, jcs258382. doi:10.1242/jcs.258382
- Camilleri-Robles, C., Amador, R., Klein, C. C., Guigó, R., Corominas, M. and Ruiz-Romero, M. (2022). Genomic and functional conservation of lncRNAs: lessons from flies. *Mamm. Genome* **33**, 328-342. doi:10.1007/s00335-021-09939-4
- Cary, G. A., Mccauley, B. S., Zueva, O., Pattinato, J., Longabaugh, W. and Hinman, V. F. (2020). Systematic comparison of sea urchin and sea star developmental gene regulatory networks explains how novelty is incorporated in early development. *Nat. Commun.* **11**, 6235. doi:10.1038/s41467-020-20023-4
- Casaca, A., Hauswirth, G. M., Bildsoe, H., Mallo, M. and Mcglinn, E. (2018). Regulatory landscape of the Hox transcriptome. *Int. J. Dev. Biol.* **62**, 693-704. doi:10.1387/ijdb.180270em
- Chen, Y. G. and Hur, S. (2022). Cellular origins of dsRNA, their recognition and consequences. *Nat. Rev. Mol. Cell Biol.* **23**, 286-301. doi:10.1038/s41580-021-00430-1
- Choi, H. M. T., Calvert, C. R., Husain, N., Huss, D., Barsi, J. C., Deverman, B. E., Hunter, R. C., Kato, M. S., Lee, M., Abelin, A. C. T. et al. (2016). Mapping a multiplexed zoo of mRNA expression. *Development* **143**, 3632-3637. doi:10.1242/dev.140137
- Corbett, A. H. (2018). Post-transcriptional regulation of gene expression and human disease. *Curr. Opin. Cell Biol.* **52**, 96-104. doi:10.1016/j.cob.2018.02.011
- Croce, J., Lhomond, G. and Gache, C. (2003). Coquille, a sea urchin T-box gene of the Tbx2 subfamily, is expressed asymmetrically along the oral-aboral axis of the embryo and is involved in skeletogenesis. *Mech. Dev.* **120**, 561-572. doi:10.1016/S0925-4773(03)00022-4
- Dahary, D., Elroy-Stein, O. and Sorek, R. (2005). Naturally occurring antisense: transcriptional leakage or real overlap? *Genome Res.* **15**, 364-368. doi:10.1101/gr.3308405
- Duboc, V., Röttinger, E., Besnardeau, L. and Lepage, T. (2004). Nodal and BMP2/4 signaling organizes the oral-aboral axis of the sea urchin embryo. *Dev. Cell* **6**, 397-410. doi:10.1016/S1534-5807(04)00056-5
- Duggan, S. P. and Mccarthy, J. V. (2016). Beyond γ -secretase activity: the multifunctional nature of presenilins in cell signalling pathways. *Cell. Signal.* **28**, 1-11. doi:10.1016/j.cellsig.2015.10.006
- Erkenbrack, E. M., Davidson, E. H. and Peter, I. S. (2018). Conserved regulatory state expression controlled by divergent developmental gene regulatory networks in echinoids. *Development* **145**, dev167288. doi:10.1242/dev.167288
- Erkenbrack, E. M., Croce, J. C., Miranda, E., Gautam, S., Martinez-Bartolome, M., Yaguchi, S. and Range, R. C. (2019). Whole mount in situ hybridization techniques for analysis of the spatial distribution of mRNAs in sea urchin embryos and early larvae. *Methods Cell. Biol.* **151**, 177-196. doi:10.1016/bs.mcb.2019.01.003
- Ettensohn, C. A. (2020). The gene regulatory control of sea urchin gastrulation. *Mech. Dev.* **162**, 103599. doi:10.1016/j.mod.2020.103599
- Ferkowicz, M. J. and Raff, R. A. (2001). Wnt gene expression in sea urchin development: heterochronies associated with the evolution of developmental mode. *Evol. Dev.* **3**, 24-33. doi:10.1046/j.1525-142x.2001.00084.x
- Fu, X.-D. (2014). Non-coding RNA: a new frontier in regulatory biology. *Natl. Sci. Rev.* **1**, 190-204. doi:10.1093/nsr/nwu008
- Godin, R. E., Urry, L. A. and Ernst, S. G. (1996). Alternative splicing of the *Endo 16* transcript produces differentially expressed mRNAs during sea urchin gastrulation. *Dev. Biol.* **179**, 148-159. doi:10.1006/dbio.1996.0247
- Gruber, A. R., Bernhart, S. H., Hofacker, I. L. and Washietl, S. (2008). Strategies for measuring evolutionary conservation of RNA secondary structures. *BMC Bioinformatics* **9**, 122. doi:10.1186/1471-2105-9-122
- Halbeisen, R. E., Galgano, A., Scherrer, T. and Gerber, A. P. (2008). Post-transcriptional gene regulation: from genome-wide studies to principles. *Cell. Mol. Life Sci.* **65**, 798-813. doi:10.1007/s00018-007-7447-6
- Hongkuan, Z., Karsoon, T., Shengkang, L., Hongyu, M. and Huaiping, Z. (2021). The functional roles of the non-coding RNAs in molluscs. *Gene* **768**, 145300. doi:10.1016/j.gene.2020.145300
- Howard-Ashby, M., Materna, S. C., Brown, C. T., Chen, L. R., Cameron, A. and Davidson, E. H. (2006). Identification and characterization of homeobox transcription factor genes in *Strongylocentrotus purpuratus*, and their expression in embryonic development. *Dev. Biol.* **300**, 74-89. doi:10.1016/j.ydbio.2006.08.039
- Istrail, S. and Peter, I. S. (2019). How does the regulatory genome work? *J. Comput. Biol.* **26**, 685-695. doi:10.1089/cmb.2019.0097
- Jakobsson, E., Argüello-Miranda, O., Chiu, S.-W., Fazal, Z., Kruczek, J., Nunez-Corrales, S., Pandit, S. and Pritchett, L. (2017). Towards a unified understanding of lithium action in basic biology and its significance for applied biology. *J. Membr. Biol.* **250**, 587-604. doi:10.1007/s00232-017-9998-2
- Kong, J. H., Yang, L., Dessaud, E., Chuang, K., Moore, D. M., Rohatgi, R., Briscoe, J. and Novitsch, B. G. (2015). Notch activity modulates the

- responsiveness of neural progenitors to sonic hedgehog signaling. *Dev. Cell* **33**, 373-387. doi:10.1016/j.devcel.2015.03.005
- Koster, M. J. E. and Timmers, H. T. M. (2015). Regulation of anti-sense transcription by Mot1p and NC2 via removal of TATA-binding protein (TBP) from the 3'-end of genes. *Nucleic Acids Res.* **43**, 143-152. doi:10.1093/nar/gku1263
- Krappinger, J. C., Bonstingl, L., Pansy, K., Sallinger, K., Wreglesworth, N. I., Grinninger, L., Deutsch, A., El-Heliebi, A., Kroneis, T., Mcfarlane, R. J. et al. (2021). Non-coding natural antisense transcripts: analysis and application. *J. Biotechnol.* **340**, 75-101. doi:10.1016/j.jbiotec.2021.08.005
- Krežel, A. and Maret, W. (2016). The biological inorganic chemistry of zinc ions. *Arch. Biochem. Biophys.* **611**, 3-19. doi:10.1016/j.abb.2016.04.010
- Kronenberg, L. H. and Humphreys, T. (1972). Double-stranded ribonucleic acid in sea urchin embryos. *Biochemistry* **11**, 2020-2026. doi:10.1021/bi00761a005
- Li, E., Materna, S. C. and Davidson, E. H. (2013). New regulatory circuit controlling spatial and temporal gene expression in the sea urchin embryo oral ectoderm GRN. *Dev. Biol.* **382**, 268-279. doi:10.1016/j.ydbio.2013.07.027
- Liang, H., Zhang, P., Bai, H.-J., Huang, J. and Yang, H.-T. (2020). TATA box-binding protein-related factor 3 drives the mesendoderm specification of human embryonic stem cells by globally interacting with the TATA box of key mesendodermal genes. *Stem Cell Res. Ther.* **11**, 196. doi:10.1186/s13287-020-01711-w
- Liu, J. A.-J. and Ngan, E. S.-W. (2014). Hedgehog and Notch signaling in enteric nervous system development. *NeuroSignals* **22**, 1-13. doi:10.1159/000356305
- Liu, Y., Beyer, A. and Aebersold, R. (2016). On the dependency of cellular protein levels on mRNA abundance. *Cell.* **165**, 535-550. doi:10.1016/j.cell.2016.03.014
- Liu, P., Song, R., Elison, G. L., Peng, W. and Acar, M. (2017). Noise reduction as an emergent property of single-cell aging. *Nat. Commun.* **8**, 680. doi:10.1038/s41467-017-00752-9
- Maret, W. (2017). Zinc in cellular regulation: the nature and significance of "Zinc Signals". *Int. J. Mol. Sci.* **18**, 2285. doi:10.3390/ijms18112285
- Marlézat, F., Couloux, A., Poulain, J., Labadie, K., Da Silva, C., Mangenot, S., Noel, B., Poustka, A. J., Dru, P., Pegueroles, C. et al. (2023). Analysis of the *P. lividus* sea urchin genome highlights contrasting trends of genomic and regulatory evolution in deuterostomes. *Cell Genomics* **3**, 100295. doi:10.1016/j.xgen.2023.100295
- McDonald, J. M. C. and Reed, R. D. (2022). Patterns of selection across gene regulatory networks. *Semin. Cell. Dev. Biol.* **145**, 60-67. doi:10.32942/OSF.IO/9ZQ7D
- McIntyre, D. C., Seay, N. W., Croce, J. C. and McClay, D. R. (2013). Short-range *Wnt5* signaling initiates specification of sea urchin posterior ectoderm. *Development* **140**, 4881-4889. doi:10.1242/dev.095844
- Morris, R. L. and Vacquier, V. D. (2019). Sea urchin embryonic cilia. *Methods Cell Biol.* **150**, 235-250. doi:10.1016/bs.mcb.2018.11.016
- Mukherjee, S., Detroja, R., Balamurali, D., Matveishina, E., Medvedeva, Y. A., Valencia, A., Gorohovski, A. and Frenkel-Morgenstern, M. (2021). Computational analysis of sense-antisense chimeric transcripts reveals their potential regulatory features and the landscape of expression in human cells. *NAR Genom Bioinform.* **3**, lqab074. doi:10.1093/nargab/lqab074
- Nojima, T. and Proudfoot, N. J. (2022). Mechanisms of lncRNA biogenesis as revealed by nascent transcriptomics. *Nat. Rev. Mol. Cell Biol.* **23**, 389-406. doi:10.1038/s41580-021-00447-6
- Oikawa, N. and Walter, J. (2019). Presenilins and γ -secretase in membrane proteostasis. *Cells* **8**, 209-241. doi:10.3390/cells8030209
- Otim, O., Amore, G., Minokawa, T., McClay, D. R. and Davidson, E. H. (2004). SpHnf6, a transcription factor that executes multiple functions in sea urchin embryogenesis. *Dev. Biol.* **273**, 226-243. doi:10.1016/j.ydbio.2004.05.033
- Otto, G. P., Sharma, D. and Williams, R. S. B. (2016). Non-catalytic roles of presenilin throughout evolution. *J. Alzheimers Dis.* **52**, 1177-1187. doi:10.3233/JAD-150940
- Pauli, A., Valen, E., Lin, M. F., Garber, M., Vastenhouw, N. L., Levin, J. Z., Fan, L., Sandelin, A., Rinn, J. L., Regev, A. et al. (2012). Systematic identification of long noncoding RNAs expressed during zebrafish embryogenesis. *Genome Res.* **22**, 577-591. doi:10.1101/gr.133009.111
- Peter, I. S. and Davidson, E. H. (2017). Assessing regulatory information in developmental gene regulatory networks. *Proc. Natl. Acad. Sci. USA* **114**, 5862-5869. doi:10.1073/pnas.1610616114
- Pfaffl, M. W. (2001). A new mathematical model for relative quantification in real-time RT-PCR. *Nucleic Acids Res.* **29**, e45. doi:10.1093/nar/29.9.e45
- Pillay, S., Takahashi, H., Carninci, P. and Kanhere, A. (2021). Antisense RNAs during early vertebrate development are divided in groups with distinct features. *Genome Res.* **31**, 995-1010. doi:10.1101/gr.262964.120
- Poustka, A. J., Kühn, A., Groth, D., Weise, V., Yaguchi, S., Burke, R. D., Herwig, R., Lehrach, H. and Panopoulou, G. (2007). A global view of gene expression in lithium and zinc treated sea urchin embryos: new components of gene regulatory networks. *Genome Biol.* **8**, R85. doi:10.1186/gb-2007-8-5-r85
- Ransick, A. (2004). Detection of mRNA by in situ hybridization and RT-PCR. *Methods Cell Biol.* **74**, 601-620. doi:10.1016/S0091-679X(04)74024-8
- Rensburg, C., Conrad, K., Sampilo, N. F. and Song, J. L. (2019). Analysis of microRNA functions. *Methods Cell Biol.* **151**, 323-334. doi:10.1016/bs.mcb.2018.10.005
- Ribas, J., Bettayeb, K., Ferandin, Y., Knockaert, M., Garrofé-Ochoa, X., Totzke, F., Schächtele, C., Mester, J., Polychronopoulos, P., Magiatis, P. et al. (2006). 7-Bromindirubin-3'-oxime induces caspase-independent cell death. *Oncogene* **25**, 6304-6318. doi:10.1038/sj.onc.1209648
- Roux, M. and Dosseto, A. (2017). From direct to indirect lithium targets: a comprehensive review of omics data. *Metallomics* **9**, 1326-1351. doi:10.1039/C7MT00203C
- Sadeq, S., Al-Hashimi, S., Cusack, C. M. and Werner, A. (2021). Endogenous double-stranded RNA. *Noncoding RNA* **7**, 15. doi:10.3390/nrna7010015
- Saudemont, A., Haillet, E., Mekpoh, F., Bessodes, N., Quirin, M., Lapraz, F., Duboc, V., Röttinger, E., Range, R., Oisel, A. et al. (2010). Ancestral regulatory circuits governing ectoderm patterning downstream of Nodal and BMP2/4 revealed by gene regulatory network analysis in an echinoderm. *PLoS Genet.* **6**, e1001259. doi:10.1371/journal.pgen.1001259
- Sethi, A. J., Angerer, R. C. and Angerer, L. M. (2009). Gene regulatory network interactions in sea urchin endomesoderm induction. *PLoS Biol.* **7**, e1000029. doi:10.1371/journal.pbio.1000029
- Smith, E. M., Pendlebury, D. F. and Nandakumar, J. (2020). Structural biology of telomeres and telomerase. *Cell. Mol. Life Sci.* **77**, 61-79. doi:10.1007/s00018-019-03369-x
- Song, J. L., Stoeckius, M., Maaskola, J., Friedländer, M., Stepicheva, N., Juliano, C., Lebedeva, S., Thompson, W., Rajewsky, N. and Wessel, G. M. (2012). Select microRNAs are essential for early development in the sea urchin. *Dev. Biol.* **362**, 104-113. doi:10.1016/j.ydbio.2011.11.015
- Statello, L., Guo, C.-J., Chen, L.-L. and Huarte, M. (2021). Gene regulation by long non-coding RNAs and its biological functions. *Nat. Rev. Mol. Cell Biol.* **22**, 96-118. doi:10.1038/s41580-020-00315-9
- Vonica, A., Weng, W., Gumbiner, B. M. and Venuti, J. M. (2000). TCF is the nuclear effector of the β -catenin signal that patterns the sea urchin animal-vegetal axis. *Dev. Biol.* **217**, 230-243. doi:10.1006/dbio.1999.9551
- Wang, L., Koppitch, K., Cutting, A., Dong, P., Kudtarkar, P., Zeng, J., Cameron, R. A. and Davidson, E. H. (2019). Developmental effector gene regulation: Multiplexed strategies for functional analysis. *Dev. Biol.* **445**, 68-79. doi:10.1016/j.ydbio.2018.10.018
- Yajima, M., Gustafson, E. A., Song, J. L. and Wessel, G. M. (2014). Piwi regulates Vasa accumulation during embryogenesis in the sea urchin. *Dev. Dyn.* **243**, 451-458. doi:10.1002/dvdy.24096
- Yao, R.-W., Wang, Y. and Chen, L.-L. (2019). Cellular functions of long noncoding RNAs. *Nat. Cell Biol.* **21**, 542-551. doi:10.1038/s41556-019-0311-8
- Yilmaz, L. S. and Noguera, D. R. (2004). Mechanistic approach to the problem of hybridization efficiency in fluorescent in situ hybridization. *Appl. Environ. Microbiol.* **70**, 7126-7139. doi:10.1128/AEM.70.12.7126-7139.2004
- Zeng, D., Chen, X., Peng, J., Yang, C., Peng, M., Zhu, W., Xie, D., He, P., Wei, P., Lin, Y. et al. (2018). Single-molecule long-read sequencing facilitates shrimp transcriptome research. *Sci. Rep.* **8**, 16920. doi:10.1038/s41598-018-35066-3
- Zhao, S., Zhang, X., Chen, S. and Zhang, S. (2020). Natural antisense transcripts in the biological hallmarks of cancer: powerful regulators hidden in the dark. *J. Exp. Clin. Cancer Res.* **39**, 187. doi:10.1186/s13046-020-01700-0
- Zucchelli, S., Fedele, S., Vatta, P., Calligaris, R., Heutink, P., Rizzu, P., Itoh, M., Persichetti, F., Santoro, C., Kawaji, H. et al. (2019). Antisense transcription in loci associated to hereditary neurodegenerative diseases. *Mol. Neurobiol.* **56**, 5392-5415. doi:10.1007/s12035-018-1465-2

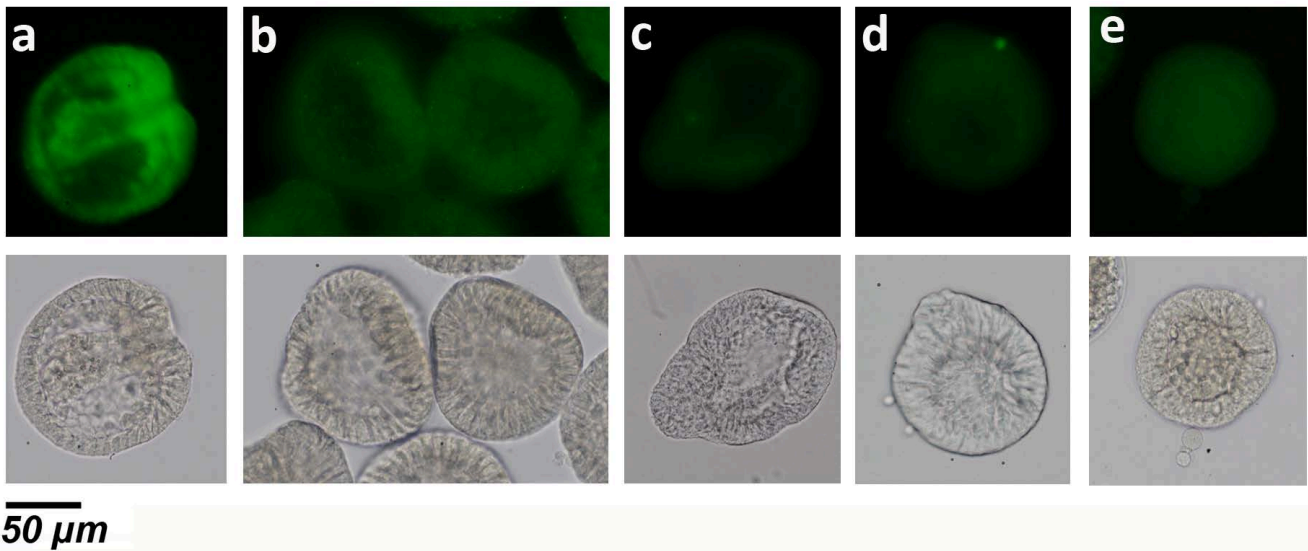


Fig. S1. IF labelling with the anti-Nter PSEN Ab. Images of IF stained embryos (upper panel) and light images (lower panel) of the same batch of 24hrs embryos either non-treated (a, control), vegetalized with LiCl (b), 5 μ M U0126 (c) or 2 μ M I0 (d) or animalized with Zn (e). As explained in Fig.1, the control gastrula is heavily stained at the vegetal side while a uniform and low staining is seen in all treated embryos.

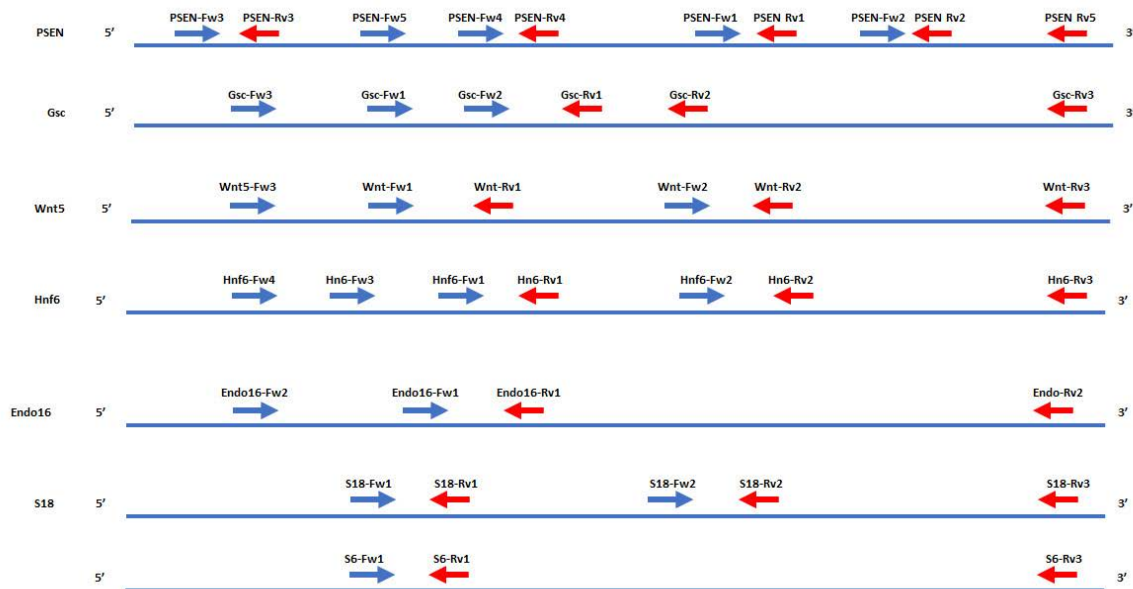


Fig. S2. Schematic representation of the positions of primers on each gene. Forward primers (blue) and reverse primers (red) whose names and sequences are listed in Table S2 are arranged on genes that are oriented 5'-3'.

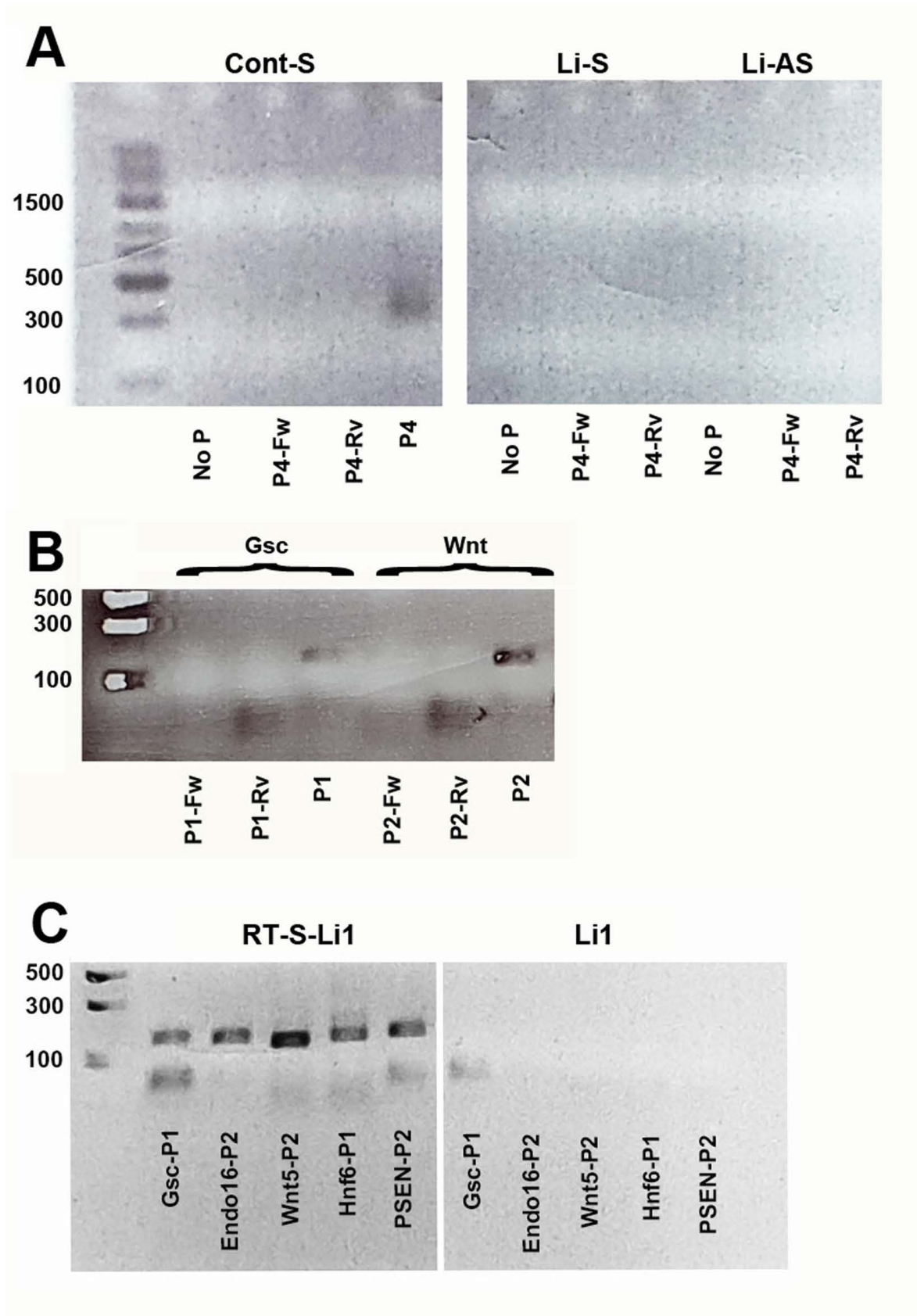


Fig. S3. Purification of sense and antisense transcripts on agarose gel after RT-PCR for sequencing. cDNAs were obtained with a combination of reverse primers (S-RT, F1-RT and F2-RT) as described in Mat and Met to detect sense (S) or antisense (F1 or F2) transcripts. We used some of the RNA preparations used for qPCR : control-Exp1 (C) , Li-Exp4 (Li) and Zn-Exp1 (Zn). PCR was run by using couples of primers as indicated on the figure. 5 μ l out of the 50 μ l of each PCR result was run on the agarose gel shown in the figure, the 45 μ l left were then run on another gel (not shown) in order to purify and sequence each band. A single band was obtained for each couple of primers at the expected size of the amplicon, all of them were purified and sequenced (Table S4) excepted those obtained with LiF1-Wnt5-P1 and Zn-F1-Gsc-P2.

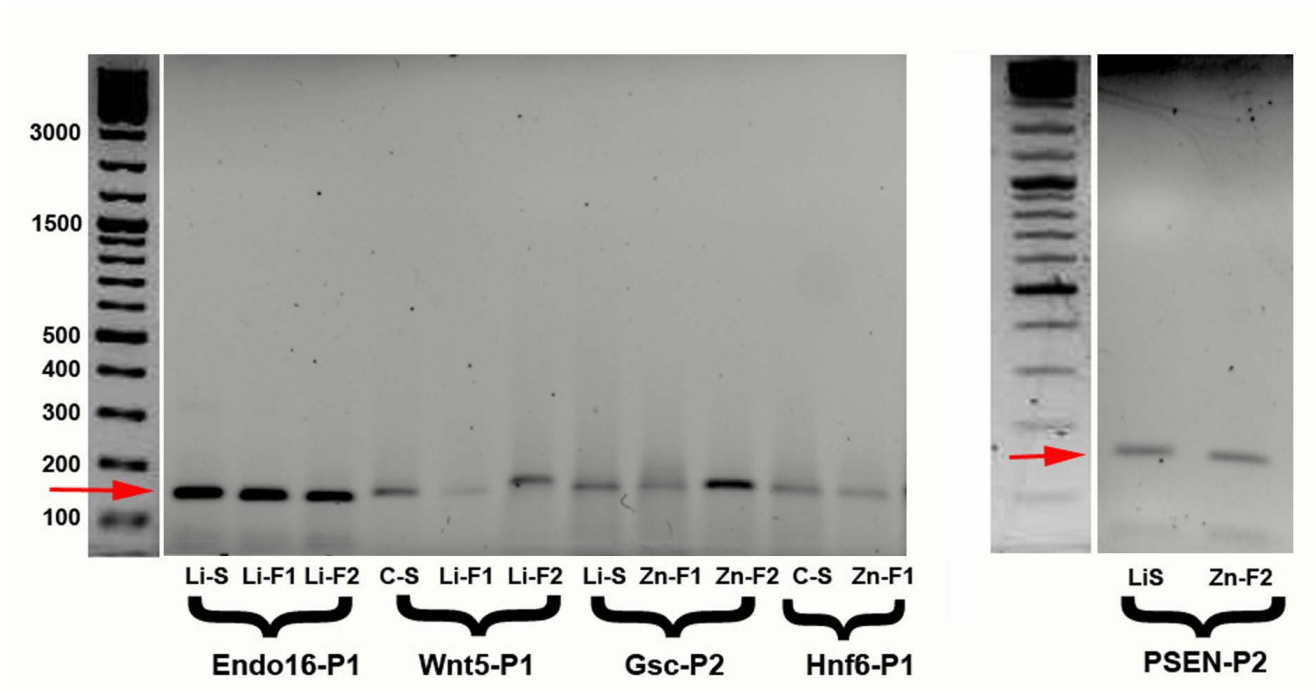


Fig. S4. Control of RT-PCR experiments

A. Control of the experiment shown in Fig. 3. RT was performed on RNA extract from 24h embryos treated or not (Cont) by LiCl (Li) and by using the primer PSEN-Rv5 or PSEN-Fw5 to detect sense (S) or antisense (AS) transcripts, respectively. No band was detected when PCR was run by using no primer (no P), P4-Fw or P4-Rv only. A band at the expected size was detected only after using the couple of primers PSEN-P4 (P4).

B. Test of Gsc and Wnt5 primers. RT was performed on RNA extract from 24h embryos treated by LiCl (Li) by using a mix of primers containing Gsc-Rv3, Wnt5-Rv3, PSEN-Rv5 and S6-Rv2. A band at the expected size was detected after PCR after using the couple of primers (P1) and none was seen by using P1-Fw or P1-Rv only.

C. Control of qPCR experiments. RT was performed on RNA extract from 24h embryos (Exp1) treated by LiCl either with the mix of primers S1-RT (RT-S-Li1) or without primers (Li1). PCR was then performed with the couples of primers as indicated on the figure. No signal was detected when RT was performed without primers.

Table S1. List of primers

Gene	Couples for PCR	Name of primer	Sequence
Endo-16	P	Endo16-Fw1	CGAGCTTGAAGACGGATGGAATT
		Endo16-Rv1	CTCCCATTCTGAACTGCCCATCA
	Endo16-Fw2	GTGTCCTTCAACTGGAAAGCG	
	Endo16-Rv2	CCTTCTGACTCTTCATCCTCCTCT	
Gsc	P1	Gsc-Fw1	GCCACCTTTGAGAAGACCCAT
		Gsc-Rv1	GCTCTCGCTTTTGCTTCCTC
	P2	Gsc-Fw2	GATGTCATGCTCAGGGAAGAACTA
		Remplacé P6	Gsc-Rv2
	Gsc-Fw3	CCCCTCGTCATCTAAGCTATCGT	
	Gsc-Fw4	GCCACCTTTGAGAAGACCCAT	
	Gsc-Rv3	CTCGTCGTCGCTGAGAAAT	
Hnf6	P1	Hnf6-Fw1	CAGGAGAATGTGGAATGGCTT
		Hnf6-Rv1	CTGGGAGGGACTCTTGGCA
	P2	Hn6-Fw2	CCGCTTTCATATTCTAACAATCA
		Hn6-Rv2	CATCAAGACAACCAACAACCAAC
	Hn6-Fw3	GTCTTACGACCCCATGGTCC	
	Hn6-Fw4	GTTTCACACACCATCACTCCCA	
	Hn6-Rv3	CACAATGCTAACTAAGCCCGACTA	
PSEN	P1	PSEN-Fw1	CGTCTCCAGCAACTCTACCTCAT
		PSEN-Rv1	CTTAGGGCATAGCACAGCAAAC
	P2	PSEN-Fw2	GAACCACCAGTAGATGATACAGCA
		PSEN-Rv2	CTGCCCTCCTGTCTTCTGATG
	P3	PSEN-Fw3	GTGGGACCAAGACGAAGACAATTCA
		PSEN-Rv3	GTTGGCCTGTCTGTTTCTTGATTG
	P4	PSEN-Fw4	AAAGCCTGGAATGCCTTGCAAATG
		PSEN-Rv4	TGAGGTAGAGTTGCTGGAGACGTAA
PSEN-Fw5		CCATTTCCACCGTTTCTTTCTAC	
PSEN Rv5		CCCTAACCCEAAATTCCTTC	
Wnt5	P1	Wnt-Fw1	CGAGGAATGCCAGAACCAGT
		Wnt-Rv1	CGACTGATAGCATTGACCACG
	P2	Wnt-Fw2	GACGCCCGCTTCAACAAA
		Wnt-Rv2	GCACCCATCGGTTCCCAT
	Wnt-Fw3	ACGACCGTCTATGACGCTACTTT	
	Wnt-Rv3	CATCGTTCAATGATCTCCTTGGT	

S6	P	S6-Fw1	GATGCGTTGAAGAGGTCACTTACTG
		S6-Rv1	GATGTCACGACGGAAGTACTCGTTT
		S6-Rv2	TTGACCTTTTGACCCCTAGATGACG
18S	P1	18S-Fw1	CTTCGTGAGGATCTGGAGCG
		18S-Rv1	CGTCTTGGTGTGCTGTCCC
	P2	18S-Fw2	CATTGATGTAACAAAGAGGGCTG
		18S-Rv2	CTTGCCGTCCTTGACATCCTT
		18S-Rv3	GCCAAATGAAAACACATCACACA

2. Mix of primers used for reverse transcriptase

S1-RT	F1-RT	F2-RT	S2-RT	F3-RT
Endo-Rv2	Endo16-Fw2	Endo16-Fw1	PSEN Rv5	PSEN-Fw3
Gsc-Rv3	Gsc-Fw3	Gsc-Fw1	S6-Rv2	S6-Rv2
Hnf6-Rv3 !	Hn6-Fw3	Hnf6-Fw1		
PSEN Rv5	PSEN-Fw3	PSEN-Fw4		
18S-Rv3	18S-Rv3	18S-Rv3		
Wnt-Rv3	Wnt5-Fw3	Wnt-Fw1		

Table S2. Raw results of control experiments obtained after qPCR analysis. All controls were analyzed with each couple of primers (Endo16-P, Hnf6-P1 and P2, Wnt5-P1 and P2 and PSEN-P1 and P2) and did not give any Ct (value=999), contrary to all sea urchin samples that gave interpretable Ct and such as S_C1_24h (Control-S-Exp1) and AS_C1_24h (Control-AS-Exp1) that are showed here as examples. For control experiments, qPCR was run after RT performed either with RNA from Li-Exp1 (C1), Zn-Exp2 (C2) or Control-Exp3 (C3) without primers or without RNA (H2O) and the mix of primers (see Table S2) S1-RT (CP1), F1-RT (CP2) or F2-RT (CP3).

Endo16		Experiment	Experiment	EvaGreen	EvaGreen	EvaGreen	EvaGreen	EvaGreen	EvaGreen	EvaGreen	EvaGreen
Chamber	Sample	EvaGreen	Ct	EvaGreen	EvaGreen	EvaGreen	EvaGreen	EvaGreen	EvaGreen	EvaGreen	EvaGreen
ID	Name	Name	Value	Calibrated	rCQuality	Call	Threshold	In Range	Tm	Peak	Rati Efficiency
S01-A09	S_C1_24h	Endo-P2	6.82929574	53.69826938		1 Pass	0.01203659	81.0361159			1 2.01779968
S25-A09	AS1_C1_24h	Endo-P2	6.724001303	57.75953673		1 Pass	0.01203659	81.13415859			1 2.01779968
S73-A09	CP1	Endo-P2	999	-1		0 Fail	0.01203659	999			0 2.01779968
S74-A09	CP2	Endo-P2	999	-1		0 Fail	0.01203659	999			0 2.01779968
S75-A09	CP3	Endo-P2	999	-1		0 Fail	0.01203659	999			0 2.01779968
S77-A09	C1	Endo-P2	999	-1		0 Fail	0.01203659	999			0 2.01779968
S78-A09	C2	Endo-P2	999	-1		0 Fail	0.01203659	999			0 2.01779968
S79-A09	C3	Endo-P2	999	-1		0 Fail	0.01203659	999			0 2.01779968
S84-A09	H2O	Endo-P2	999	-1		0 Fail	0.01203659	999			0 2.01779968
Hnf6-P2											
S01-A08	S_C1_24h	Hnf-P2	9.316810242	509.8860417		1 Pass	0.009124301	76.16367109			1 2.026508671
S25-A08	AS1_C1_24h	Hnf-P2	12.876420514	42.50101914		1 Pass	0.009124301	76.21657339			1 2.026508671
S73-A08	CP1	Hnf-P2	999	-1		0 Fail	0.009124301	999			0 2.026508671
S74-A08	CP2	Hnf-P2	999	-1		0 Fail	0.009124301	999			0 2.026508671
S75-A08	CP3	Hnf-P2	999	-1		0 Fail	0.009124301	999			0 2.026508671
S77-A08	C1	Hnf-P2	999	-1		0 Fail	0.009124301	999			0 2.026508671
S78-A08	C2	Hnf-P2	999	-1		0 Fail	0.009124301	999			0 2.026508671
S79-A08	C3	Hnf-P2	999	-1		0 Fail	0.009124301	999			0 2.026508671
S84-A08	H2O	Hnf-P2	999	-1		0 Fail	0.009124301	999			0 2.026508671
Hnf6-P1											
S01-A07	S_C1_24h	Hnf-P1	10.80715028	169.5170921		1 Pass	0.010011536	86.24522552			1 1.899116172
S25-A07	AS1_C1_24h	Hnf-P1	12.25362654	67.21262256		1 Pass	0.010011536	86.34009428			1 1.899116172
S73-A07	CP1	Hnf-P1	999	-1		0 Fail	0.010011536	999			0 1.899116172
S74-A07	CP2	Hnf-P1	999	-1		0 Fail	0.010011536	999			0 1.899116172
S75-A07	CP3	Hnf-P1	999	-1		0 Fail	0.010011536	999			0 1.899116172
S77-A07	C1	Hnf-P1	999	-1		0 Fail	0.010011536	999			0 1.899116172
S78-A07	C2	Hnf-P1	999	-1		0 Fail	0.010011536	999			0 1.899116172
S79-A07	C3	Hnf-P1	999	-1		0 Fail	0.010011536	999			0 1.899116172
S84-A07	H2O	Hnf-P1	999	-1		0 Fail	0.010011536	999			0 1.899116172
Wnt5-P2											
S01-A06	S_C1_24h	Wnt-P2	10.06752665	299.0454171		1 Pass	0.00833054	84.9962557			1 1.968419447
S25-A06	AS1_C1_24h	Wnt-P2	13.86705505	22.88732146		1 Pass	0.00833054	84.92357406			1 1.968419447
S73-A06	CP1	Wnt-P2	999	-1		0 Fail	0.00833054	999			0 1.968419447
S74-A06	CP2	Wnt-P2	999	-1		0 Fail	0.00833054	999			0 1.968419447
S75-A06	CP3	Wnt-P2	999	-1		0 Fail	0.00833054	999			0 1.968419447
S77-A06	C1	Wnt-P2	999	-1		0 Fail	0.00833054	999			0 1.968419447
S78-A06	C2	Wnt-P2	999	-1		0 Fail	0.00833054	999			0 1.968419447
S79-A06	C3	Wnt-P2	999	-1		0 Fail	0.00833054	999			0 1.968419447
S84-A06	H2O	Wnt-P2	999	-1		0 Fail	0.00833054	999			0 1.968419447
Wnt5-P1											
S01-A05	S_C1_24h	Wnt-P1	10.96577282	100.391239		1 Pass	0.010000629	82.9172744			1 1.82430146
S25-A05	AS1_C1_24h	Wnt-P1	13.41582387	23.0878649		1 Pass	0.010000629	82.88302283			1 1.82430146
S73-A05	CP1	Wnt-P1	999	-1		0 Fail	0.010000629	999			0 1.82430146
S74-A05	CP2	Wnt-P1	999	-1		0 Fail	0.010000629	999			0 1.82430146
S75-A05	CP3	Wnt-P1	999	-1		0 Fail	0.010000629	999			0 1.82430146
S77-A05	C1	Wnt-P1	999	-1		0 Fail	0.010000629	999			0 1.82430146
S78-A05	C2	Wnt-P1	999	-1		0 Fail	0.010000629	999			0 1.82430146
S79-A05	C3	Wnt-P1	999	-1		0 Fail	0.010000629	999			0 1.82430146
S84-A05	H2O	Wnt-P1	999	-1		0 Fail	0.010000629	999			0 1.82430146
Gsc-P2											
S01-A04	S_C1_24h	Gsc-P2	11.99574741	220.9043012		1 Pass	0.009053902	84.96609506			1 1.80199871
S25-A04	AS1_C1_24h	Gsc-P2	13.30754905	101.9186552		1 Pass	0.009053902	85.23727489			1 1.80199871
S73-A04	CP1	Gsc-P2	999	-1		0 Fail	0.009053902	999			0 1.80199871
S74-A04	CP2	Gsc-P2	999	-1		0 Fail	0.009053902	999			0 1.80199871
S75-A04	CP3	Gsc-P2	999	-1		0 Fail	0.009053902	999			0 1.80199871
S77-A04	C1	Gsc-P2	999	-1		0 Fail	0.009053902	999			0 1.80199871
S78-A04	C2	Gsc-P2	999	-1		0 Fail	0.009053902	999			0 1.80199871
S79-A04	C3	Gsc-P2	999	-1		0 Fail	0.009053902	999			0 1.80199871
S84-A04	H2O	Gsc-P2	999	-1		0 Fail	0.009053902	999			0 1.80199871
Gsc-P1											
S01-A03	S_C1_24h	Gsc-P1	12.49405968	153.1413783		1 Pass	0.010295008	82.22658156			1 1.863246312
S25-A03	AS1_C1_24h	Gsc-P1	12.8140121	125.4496333		1 Pass	0.010295008	82.28024335			1 1.863246312
S73-A03	CP1	Gsc-P1	999	-1		0 Fail	0.010295008	999			0 1.863246312
S74-A03	CP2	Gsc-P1	999	-1		0 Fail	0.010295008	999			0 1.863246312
S75-A03	CP3	Gsc-P1	999	-1		0 Fail	0.010295008	999			0 1.863246312
S76-A03	C12	Gsc-P1	999	-1		0 Fail	0.010295008	999			0 1.863246312
S77-A03	C1	Gsc-P1	999	-1		0 Fail	0.010295008	999			0 1.863246312
S78-A03	C2	Gsc-P1	999	-1		0 Fail	0.010295008	999			0 1.863246312
S79-A03	C3	Gsc-P1	999	-1		0 Fail	0.010295008	999			0 1.863246312
S84-A03	H2O	Gsc-P1	999	-1		0 Fail	0.010295008	999			0 1.863246312
PSEN-P2											
S01-A02	S_C1_24h	PSEN-P2	10.96403516	48.52548997		1 Pass	0.008864765	81.70822247			1 1.899116172
S25-A02	AS1_C1_24h	PSEN-P2	13.72831489	8.252617757		1 Pass	0.008864765	81.84135906			1 1.899116172
S73-A02	CP1	PSEN-P2	999	-1		0 Fail	0.008864765	999			0 1.899116172
S74-A02	CP2	PSEN-P2	999	-1		0 Fail	0.008864765	999			0 1.899116172
S77-A02	C6	PSEN-P2	999	-1		0 Fail	0.008864765	999			0 1.899116172
S78-A02	C14	PSEN-P2	999	-1		0 Fail	0.008864765	999			0 1.899116172
S79-A02	C23	PSEN-P2	999	-1		0 Fail	0.008864765	999			0 1.899116172
S84-A02	H2O	PSEN-P2	999	-1		0 Fail	0.008864765	999			0 1.899116172
PSEN-P1											
S01-A01	S_C1_24h	PSEN-P1	11.54335391	42.02690365		1 Pass	0.009278142	81.33743495			1 1.923494324
S25-A01	AS1_C1_24h	PSEN-P1	14.45000507	6.291703637		1 Pass	0.009278142	81.68788278			1 1.923494324
S73-A01	CP1	PSEN-P1	999	-1		0 Fail	0.009278142	999			0 1.923494324
S74-A01	CP2	PSEN-P1	999	-1		0 Fail	0.009278142	999			0 1.923494324
S75-A01	CP3	PSEN-P1	999	-1		0 Fail	0.009278142	999			0 1.923494324
S77-A01	C1	PSEN-P1	999	-1		0 Fail	0.009278142	999			0 1.923494324
S78-A01	C2	PSEN-P1	999	-1		0 Fail	0.009278142	999			0 1.923494324
S79-A01	C3	PSEN-P1	999	-1		0 Fail	0.009278142	999			0 1.923494324
S84-A01	H2O	PSEN-P1	999	-1		0 Fail	0.009278142	999			0 1.923494324

Table S3. Sequences of Plasmids used in this study

<p>Gsc in pBlueScript</p> <p>5'ACTCACTATAGGGCAAGCAGTGGTAACAACGCAGAGTACGCGGGGATTGACAAGATAAAAT TATAAAAGCTGGTGCGACAACTGACACAATCTCAGAGTGGAATAGTTTCTTATTTTCATATATCG TCCTAAGTGGTTAGCTCTGATCTTTGAGATGGACTATTACCTTCCAGACATCGCTCCAGCAGGCC GCCTCACCATGAACGCCGCGTCGATCCTCGCTGCTGGTCTTCCCCGCTCGGATCACAGTCCCTCA TCACCTCCATCATCATCACCATTAGCATCGTCTCCACCAGCGACACCTACATCATCCCCCTCGTC ATCTAAGTACCGTTCTCGTCCTCGCCGATCTCCCCGGCCATGGCAGGCTACTACAACCCTTACA CCGGCTGCCCCATGACGGGCATGACGAGTCCATCGTTCACCATCGACAACATTTTGGCGCCTCGT CCCTACCCGGCTGTGCCCCGCGGCATGCTCCCTATCTACCGCTAACTCCGCACCCTCACTTCCC CTACTTCATCCCAGTACCACCTAGCTGCCTACCATGCCTACTCAGCCTACCCCCACATGGATCT GATAGCTCGTAATCAAAAGAGAAAGCGACGTCATCGTACTATATTTCACTGAAGAGCAACTTGAA CAACTGGAAGCCACCTTTGAGAAGACCCATTATCCCGATGTCATGCTCAGGGAAGAACTAGCAA TCAAAGTCGATCTCAAAGAAGAACGAGTCGAGGTTTGGTTCAAAGAACC GCCGCTAAGTGGAG GAAGCAAAGCGAGAGCAACAAGAGGCTGCCAAGCGTGCTTCCGAGGTGTACAAGAAAGAGTA CGGATCTAATCCGGACAAACCATCCACTAGCACTACGACAACGACATCATCTCGGCCAACTTCA CAATCATCTCTCGACTCGTACCCGTCATCGATGGATGATAGAAACCGCGTCACTTCAGAC 3'</p>
<p>Wnt5 in pBlueScript</p> <p>5'TACGAACCTCCTTATCGAGTCACTCTCCGTCTGCCAGCACTTGCAGGAACTTGACGTTGAATCGG AGATCGCAGACTTCTTGGACGATAAGTCGACGGTTTTCCCGTCTCCTTCGACGACCGTCTATGAC GCTACTTCAAACGCCTTAATCTTACTGTGGACTTTTGTGGAATTTTATCACCATCACTTACGAG AGCACAAGATACAACATGGATAAATCTAGGACTGGACACACGAGTGCAGCAGTTCGATGCCTTC CGTAACCCTGAGCTGTTCACTCCTGGGCACCCAGCCCCTGTGCAGTGAGTTACTGGGTCTGTCACC TGGTCAGCAGAACTGTGCCAACTCTACCAGGACCACATGGCACCCATAGGCCGAAGGAGCCAA GATGAGTATCGAGGAATGCCAGAACCAGTTTLAGGAATAGGAGGTGGAAGTGCAGCACTGTTGAT AGCAATAATGTCTTCGGGAAAGTGCTCAGCATATCGAGTCGTGAAGCAGCGTTCACCTTATGCCA TCACTTCAGCAGGCGTGGTCAATGCTATCAGTCGGTCGTGCAGGGAAGGACAGCTATCAACATG TGGATGTGGCAAGTCAGCACGTCCAGATGACATCCCTCGCGACTGGGTGTGGGGAGGGTGC GACAACATCGACTACGGCTTCCGTTTCGCCCGGAGTTCGTCGATGCTCGGGAGATGGAGACCA ACCCTCAACGAGGAAGCTACGCTTATAGTCGCATGAAGATGAAGTACATAACAATGAAGCTGG TAGAAAGGCGGTTTATGATAACCGCTTGGTACCGAATGCAAATTGCCATG 3'</p>

<p>Gsc-S</p>	<p>Li treated embryos, Exp2, S1-RT</p>	<p>Gsc-P2 Li-S on gel</p>	<p>Gsc-Rv2</p>	<p>>Pliv04889.1 gene=Gsc CDS=220-1209, Length = 2390, Identities = 111/112 (99%)</p> <p>Query: gttgttttcgcttttgcttccctcacttagcgcgggcggttcttgaaccaaactcgactc Sbjct: gttgttctcgcttttgcttccctcacttagcgcgggcggttcttgaaccaaactcgactc Query: gttcttctttgagatcgactttgattgctagttcttccctgagcatgacatc Sbjct: gttcttctttgagatcgactttgattgctagttcttccctgagcatgacatc</p> <p><u>gatgtcatgctcagggagaactagcaatcaaagtcgatctcaaagaagaacgagtcgaggtttggttcaa</u> <u>gaaccgccgcgctaagtggaggaagcaaaagcgagagccacaagaggctgccaagcgtgcttccgaggtgt</u> <u>ac</u></p>
<p>Gsc-AS</p>	<p>Zn treated embryos, Exp1, F2-RT</p>	<p>Gsc-P2 Zn-F2 on gel</p>	<p>Gsc-Fw2</p> <p>Gsc-Rv2</p>	<p>>Pliv04889.1 gene=Gsc CDS=220-1209, Length = 2390, Identities = 92/93 (98%)</p> <p>Query: acgagtcgaggtttggttcaagaaccgccgcgctaagtggaggaagcaaaagcgagagca Sbjct: acgagtcgaggtttggttcaagaaccgccgcgctaagtggaggaagcaaaagcgagaaca Query: acaagaggctgccaagcgtgcttccgaggtgta Sbjct: acaagaggctgccaagcgtgcttccgaggtgta</p> <p>>Pliv04889.1 gene=Gsc CDS=220-1209, Length = 2390, Identities = 107/107 (100%)</p> <p>Query: tctcgcttttgcttccctcacttagcgcgggcggttcttgaaccaaactcgactcgttct Sbjct: tctcgcttttgcttccctcacttagcgcgggcggttcttgaaccaaactcgactcgttct Query: tctttgagatcgactttgattgctagttcttccctgagcatgacatc Sbjct: tctttgagatcgactttgattgctagttcttccctgagcatgacatc</p> <p><u>gatgtcatgctcagggagaactagcaatcaaagtcgatctcaaagaagaacgagtcgaggtttggttcaa</u> <u>gaaccgccgcgctaagtggaggaagcaaaagcgagagccacaagaggctgccaagcgtgcttccgaggtgt</u> <u>ac</u></p>

<p>Wnt5-S</p>	<p>Control embryos, Exp1, S1-RT</p>	<p>Wnt5-P1 C-S on gel</p>	<p>Wnt5-Rv1</p>	<p>>Pliv24335.1 gene=Wnt5 CDS=1-885, Length = 885, Identities = 89/90 (98%)</p> <p>Query: atatgctgagcaccttcccccaagacattattgctatcaacagtgctgcagttccacctcc Sbjct: atatgctgagcaccttcccgaagacattattgctatcaacagtgctgcagttccacctcc Query: tattcctaaactggttctggcattcctcga Sbjct: tattcctaaactggttctggcattcctcga</p> <p><u>cgaggaatgccagaaccagtttaggaataggaggtggaactgcagcactgttgatagcaataatgtcttcg</u> <u>ggaagtgctcagcatatcgagtcgtgaagcagcgttcacctatgcatcacttcagcaggcgtggtcaat</u> <u>gctatcagtcgg</u></p>
<p>Wnt5-AS</p>	<p>Li treated embryos, Exp2, F2-RT</p>	<p>Wnt5-P1 Li-F2 on gel</p>	<p>Wnt5-Fw1</p> <p>Wnt5-Rv1</p>	<p>>Pliv25410.1 gene=Wnt5 CDS=1-789, Length = 789, Identities = 64/64 (100%)</p> <p>Query: cgagtcgtgaagcagcgttcacctatgcatcacttcagcaggcgtggtcaatgctatca Sbjct: cgagtcgtgaagcagcgttcacctatgcatcacttcagcaggcgtggtcaatgctatca Query: gtcg Sbjct: gtcg</p> <p>>Pliv24335.1 gene=Wnt5 CDS=1-885, Length = 885, Identities = 90/90 (100%)</p> <p>Query: atatgctgagcaccttcccgaagacattattgctatcaacagtgctgcagttccacctcc Sbjct: atatgctgagcaccttcccgaagacattattgctatcaacagtgctgcagttccacctcc Query: tattcctaaactggttctggcattcctcga Sbjct: tattcctaaactggttctggcattcctcga</p> <p><u>cgaggaatgccagaaccagtttaggaataggaggtggaactgcagcactgttgatagcaataatgtcttcg</u> <u>ggaagtgctcagcatatcgagtcgtgaagcagcgttcacctatgcatcacttcagcaggcgtggtcaat</u> <u>gctatcagtcgg</u></p>

